

Globally Solving Concave Quadratic Programs via Doubly Nonnegative Relaxation

Zheng Qu · Tianyou Zeng · Yuchen Lou

Abstract We consider the problem of maximizing a convex quadratic function over a bounded polyhedral set. We design a new framework based on SDP relaxations and cutting plane methods for solving the associated reference value problem. The major novelty is a new way to generate valid cuts through the doubly nonnegative (DNN) relaxation. We establish various theoretical properties of the DNN relaxation, including its equivalence with the Shor relaxation of an equivalent quadratically constrained problem, the strong duality, and the generation of valid cuts from an approximate solution of the DNN relaxation returned by an arbitrary SDP solver. Computational results on both real and synthetic data demonstrate the efficiency of the proposed method and its ability to solve high-dimensional problems with dense data. In particular, our new algorithm successfully solves in 3 days the reference value problem arising from computational biology for a dataset containing more than 300,000 instances of dimension 78. In contrast, CPLEX or Gurobi is estimated to require years of computational time for the same dataset on the same computing platform.

Keywords Concave quadratic programming · Doubly nonnegative relaxation · Cutting plane method · Strong duality · Valid bound · Large-scale nonconvex programming

Mathematics Subject Classification (2020) 90C20 · 90C22 · 90C26 · 90C59

Z. Qu
School of Mathematical Sciences, Shenzhen University.
E-mail: quzheng2003@gmail.com

T. Zeng
Department of Mathematics, The University of Hong Kong.
E-mail: logic@connect.hku.hk

Y. Lou
Department of Industrial Engineering and Management Sciences, Northwestern University.
E-mail: yuchenlou2026@u.northwestern.edu

1 Introduction

1.1 Background

We consider the following problem of maximizing a convex quadratic function over a polyhedral set:

$$\begin{aligned} \Phi^*(\mathcal{F}) &:= \max_{y \in \mathbb{R}^k} && \Phi(y) \\ &\text{s.t.} && y \in \mathcal{F}. \end{aligned} \quad (1)$$

Here,

$$\Phi(y) \equiv y^\top Q y + 2d^\top y + \nu$$

is a convex quadratic function, where $Q \in \mathbb{R}^{k \times k}$ is a positive semidefinite matrix, $d \in \mathbb{R}^k$ is a vector and $\nu \in \mathbb{R}$ is a scalar. The feasible region \mathcal{F} is a polyhedral set written in the following form:

$$\mathcal{F} := \{y \in \mathbb{R}^k : F^\top y \leq w, y \geq 0\}, \quad (2)$$

where $F \in \mathbb{R}^{k \times m}$ and $w \in \mathbb{R}^m$. We further assume that \mathcal{F} has nonempty interior and is bounded. Note that problem (1) is equivalent to minimizing a concave quadratic function over a polyhedral set. For this reason, we shall refer to problem (1) as a concave quadratic program (QP).

Concave QP has important applications in many areas, including engineering [9,23], industry [1,4] and medical diagnosis [7,21]. More recently, concave QP finds new applications in computational biology [15,39]. The biology problem concerned is the detection of undiscovered protein/genome sequence and a key step in the approach proposed in [15,39] consists in solving the following problem:

$$\text{determine whether } \nu_R > \Phi^*(\mathcal{F}) \text{ or } \Phi^*(\mathcal{F}) \geq \nu_R ? \quad (3)$$

Here, ν_R is a certain prescribed reference value. For convenience, we shall refer to (3) as the *reference value problem* associated with the concave QP problem (1). In this real application, m is fixed to 22 and the number of known protein/genome sequences of a certain species is equal to $m + k$. Depending on the species considered, the dimension k or the number of reference value problems may be very large. For example, we have access to a dataset with 317,584 instances of dimension $k = 78$, and a dataset with 3 instances of dimension $k = 819$. The new protein detection problem requires one to solve the reference value problem for **all** the instances in the dataset.

We randomly selected 100 instances from the 317,584 instances of dimension $k = 78$, and employed two off-the-shelf commercial solvers **Cplex** and **Gurobi** to solve them. The time limit was set as 600 seconds for both solvers. The results show that **Cplex** fails to give an answer to the reference value problem (3) on 92 instances, and **Gurobi** fails on 48 instances. The performance of both **Cplex** and **Gurobi** clearly does not make the grade, as the computational time of solving all 317,584 instances using **Cplex** or **Gurobi** is estimated to be

at least 3 years¹. Moreover, the 3 instances of dimension $k = 819$ cannot be handled by CPLEX nor Gurobi due to the large dimension.

Motivated by the challenges raised above, we develop in this paper a new method for solving the reference value problem (3) associated with the concave QP problem (1). This new method can also be naturally extended to a global solver of (1). We focus on the efficiency of the algorithm for large dimensional problems. In particular, the algorithm should be highly efficient so that the 317,584 instances of dimension $k = 78$ can be solved in a reasonable amount of time. Moreover, the algorithm should be able to deal with high-dimensional problems so that instances of dimension up to $k = 819$ can be handled as well.

1.2 Related work

Problem (1) falls into the class of general nonconvex QP problems. There are three major techniques to find a global solution of general QP problems: reformulation, branching, and relaxation [19,25]. QP problems can be reformulated in different ways, including bilinear reformulation [17,18], KKT reformulation [3,6], completely positive reformulation [2], and mixed-integer LP reformulation [8,37]. After certain reformulation of the QP according to the problem structures, branch-and-bound (B&B) algorithms are employed in nearly all the state-of-the-art global QP solvers. There exist various branching strategies based on different reformulations [6,37]. Importantly, the efficiency of the bounding step crucially depends on the quality of the relaxations utilized. Well-known relaxations include, for example, McCormick relaxation [22], semidefinite programming (SDP) relaxation [20,24], convex quadratic relaxation by separable programming or DC (difference of convex functions) programming [12], and doubly nonnegative relaxation [2].

Regarding the concave QP problem (1), it has also been extensively studied in the literature and is known to be an NP-hard problem [27]. Traditional methods mainly include enumerative methods [5], cutting plane methods [18,33], successive approximation methods (see Chapter 6 in [13]), and branch-and-bound methods [3,6]. Details and references for early work on concave QP can be found in the survey paper of Pardalos and Rosen [26] and in the book of Horst and Tuy [13]. More recently, Zamani [38] proposed a method which combines the cutting plane method and the branch-and-bound method for concave QP. Telli et al. [31] proposed to approximate the global optimum by solving a sequence of linear programs constructed from a local approximation set. Hladik et al. [10,11] proposed new bounds for concave QP based on factorization.

¹ If half of the instances require at least 600 seconds to solve on average, in total we need at least $600 \times 317584/2 = 95275200$ seconds, which is roughly 3 years.

1.3 Review on the doubly nonnegative relaxation

In this section, we recall the concept of the doubly nonnegative (DNN) relaxation of a QP. We first reformulate the original QP (1) into an equivalent form with linear equality constraints. Let $n = m + k$. One can lift the feasible region \mathcal{F} into \mathbb{R}^n and rewrite (1) in the following form:

$$\begin{aligned} \max_{x \in \mathbb{R}^n} \quad & x^\top \begin{pmatrix} Q & \mathbf{0} \\ \mathbf{0}^\top & 0 \end{pmatrix} x + 2(d^\top \mathbf{0}^\top) x + \nu \\ \text{s.t.} \quad & (F^\top \mathbf{I}) x = w \\ & x \geq 0. \end{aligned} \quad (4)$$

In problem (4) above, $\mathbf{0}$ denotes the zero vector or matrix of appropriate dimension, and \mathbf{I} denotes the identity matrix of appropriate dimension. A square matrix is completely positive (CP) if it can be written as BB^\top where B is a matrix with nonnegative elements only. It is known, given in the theorem below, that problem (4) can be reformulated as a linear program over the cone of CP matrices.

Theorem 1 ([2]) *The quadratic program (4) is equivalent to*

$$\begin{aligned} \max_{\substack{X \in \mathcal{S}^n \\ x \in \mathbb{R}^n}} \quad & \left\langle \begin{pmatrix} Q & \mathbf{0} \\ \mathbf{0}^\top & 0 \end{pmatrix}, X \right\rangle + 2(d^\top \mathbf{0}^\top) x + \nu \\ \text{s.t.} \quad & (F^\top \mathbf{I}) x = w \\ & \text{diag} \left((F^\top \mathbf{I}) X \begin{pmatrix} F \\ \mathbf{I} \end{pmatrix} \right) = w \circ w \\ & \begin{pmatrix} X & x \\ x^\top & 1 \end{pmatrix} \in \mathcal{C}_{n+1}. \end{aligned} \quad (5)$$

Here, \circ denotes the operation of the element-wise product of two vectors, \mathcal{S}^n is the space of n -by- n symmetric matrices and \mathcal{C}_{n+1} is the cone of $(n+1)$ -by- $(n+1)$ completely positive matrices:

$$\mathcal{C}_{n+1} = \left\{ BB^\top : B \in \mathbb{R}_+^{(n+1) \times \ell}, \ell \in \mathbb{N} \right\}.$$

The CP cone \mathcal{C}_{n+1} can be approximated from the outside by a hierarchy of cones of linear- and semidefinite-representable cones $\mathcal{D}_0 \supset \mathcal{D}_1 \supset \dots \supset \mathcal{C}_{n+1}$, with \mathcal{D}_0 corresponding to the cone of doubly nonnegative (DNN) matrices, i.e., the matrices that are positive semidefinite and elementwisely nonnegative. Replacing \mathcal{C}_{n+1} by \mathcal{D}_0 , we obtain the following *doubly nonnegative relaxation*

of (4):

$$\begin{aligned}
 \bar{\Phi}(\mathcal{F}) := \max_{\substack{X \in \mathcal{S}^n \\ x \in \mathbb{R}^n}} & \left\langle \begin{pmatrix} Q & \mathbf{0} \\ \mathbf{0}^\top & 0 \end{pmatrix}, X \right\rangle + 2 (d^\top \mathbf{0}^\top) x + \nu \\
 \text{s.t.} & (F^\top \mathbf{I}) x = w \\
 & \text{diag} \left((F^\top \mathbf{I}) X \begin{pmatrix} F \\ \mathbf{I} \end{pmatrix} \right) = w \circ w \\
 & \begin{pmatrix} X & x \\ x^\top & 1 \end{pmatrix} \succeq 0, \quad \begin{pmatrix} X & x \\ x^\top & 1 \end{pmatrix} \preceq 0.
 \end{aligned} \tag{6}$$

It is easy to see that:

$$\bar{\Phi}(\mathcal{F}) \geq \Phi^*(\mathcal{F}). \tag{7}$$

In the following we refer to (6) as the DNN relaxation of (4), and $\bar{\Phi}(\mathcal{F})$ as the DNN bound of $\Phi^*(\mathcal{F})$. Note that (6) is a semidefinite program (SDP) and can be solved numerically by several existing SDP solvers, e.g. [30,32,36]. There are also efficient solvers specially dedicated to approximate the DNN bound $\bar{\Phi}(\mathcal{F})$, e.g. [16].

1.4 Approach and contribution

We summarize in this subsection the main routine of our proposed algorithm and its novelty.

A vector $\bar{y} \in \mathcal{F}$ is a Karush–Kuhn–Tucker (KKT) point of (1) if it satisfies

$$\begin{aligned}
 0 = \max & \quad \langle \nabla \Phi(\bar{y}), y - \bar{y} \rangle \\
 \text{s.t.} & \quad y \in \mathcal{F}.
 \end{aligned} \tag{8}$$

A vector $\bar{y} \in \mathcal{F}$ is said to be a *KKT vertex* if \bar{y} is both a vertex of the polyhedral set \mathcal{F} and a KKT point of (1). Note that any optimal solution of (1) must be a KKT point, and at least one optimal solution of (1) is a vertex of \mathcal{F} .

In the proposed method, we start by searching for a KKT vertex \bar{y} of (1). If $\Phi(\bar{y}) \geq \nu_R$, we conclude that $\Phi^*(\mathcal{F}) \geq \nu_R$ and the reference value problem (3) is solved. If $\Phi(\bar{y}) < \nu_R$, we compute the DNN bound $\bar{\Phi}(\mathcal{F})$ defined by (6). If

$$\bar{\Phi}(\mathcal{F}) < \nu_R, \tag{9}$$

we conclude that $\Phi^*(\mathcal{F}) < \nu_R$ and the reference value problem is solved. If instead $\bar{\Phi}(\mathcal{F}) \geq \nu_R$, we propose to rely on the classical cutting plane method to proceed.

We will iteratively add valid cuts to the original problem (1) so that the feasible region is reduced successively until we find an answer to (3). The major novelty of our approach is the computation of valid cuts from the DNN relaxation. Let \bar{y} be a KKT vertex of the QP problem (1) such that $\Phi(\bar{y}) < \nu_R$. If there is a region $\Delta \ni \bar{y}$ such that

$$\nu_R > \Phi^*(\mathcal{F} \cap \Delta) := \max\{\Phi(y) : y \in \mathcal{F} \cap \Delta\}, \tag{10}$$

then we only need to consider the restricted region $\mathcal{F} \setminus \Delta$ instead of \mathcal{F} to find an answer to (3). We shall search for a region $\Delta \ni \bar{y}$ such that (10) holds and a valid cut can be added to describe the restricted region $\mathcal{F} \setminus \Delta$. This cut will exclude a region which contains the KKT point \bar{y} . Therefore, we can continue to deal with a concave QP problem with a strictly smaller feasible region $\mathcal{F} \setminus \Delta$, and the same process is repeated until an answer to (3) is obtained.

It is interesting to note that (10) is in fact a reference value problem defined in (3). Directly verifying (10) being difficult, it is common to replace $\Phi^*(\mathcal{F} \cap \Delta)$ in (10) by a computable upper bound of it. In [33], Tuy proposed to generate a valid cut using the following computable upper bound of $\Phi^*(\mathcal{F} \cap \Delta)$:

$$\max\{\Phi(y) : y \in \Delta\}.$$

In [18], Konno proposed another computable upper bound of $\Phi^*(\mathcal{F} \cap \Delta)$:

$$\bar{\Phi}^K(\mathcal{F} \cap \Delta) := \max\{\Psi(y, \tilde{y}) : y \in \Delta, \tilde{y} \in \mathcal{F}\}, \quad (11)$$

where $\Psi(y, \tilde{y}) := y^\top Q \tilde{y} + d^\top y + d^\top \tilde{y} + \nu$. In this paper, we propose to employ the DNN bound $\bar{\Phi}(\mathcal{F})$ and validate (10) by the following condition:

$$\bar{\Phi}(\mathcal{F} \cap \Delta) < \nu_R. \quad (12)$$

We show that the cut generated by our method is always deeper than Konno's cut, by proving in Theorem 2 that

$$\bar{\Phi}(\mathcal{F} \cap \Delta) \leq \bar{\Phi}^K(\mathcal{F} \cap \Delta). \quad (13)$$

The computation of the DNN bounds in (9) and (12) clearly plays a decisive role in the overall performance of the procedure described above. With the goal of developing an efficient and robust concave QP solver in the large-scale setting, we also tackle the following two problems:

1. It is known that the SDP problems in the form of (6) do not have an interior point (see Proposition 8.3 and the last paragraph of Section 8.2.2 in [2]). However, the theoretical convergence of the existing popular SDP solvers (e.g. [30, 32, 36]) is established with the assumption of Slater's condition, i.e., the existence of an interior point.
2. Any numerical solver using finite floating-point arithmetic is incapable of returning the exact value of $\bar{\Phi}(\mathcal{F})$. Let ν be the value returned by a numerical SDP solver (e.g. MOSEK and SDPNAL+ [30]) when solving (6). Then ν is an approximation (whatever the precision is) of $\bar{\Phi}(\mathcal{F})$. In particular, $\nu < \nu_R$ does not necessarily imply (9). A similar problem also occurs for computing $\bar{\Phi}(\mathcal{F} \cap \Delta)$ and verifying (12).

To address the first issue, we prove in Lemma 1 that the DNN relaxation (6) has an equivalent SDP formulation (15), which corresponds to the Shor relaxation applied to an equivalent quadratically constrained quadratic program (QCQP) of (1). We then show in Proposition 1 that under some mild assumptions, Slater's condition holds for (15), and hence all the above-mentioned

SDP solvers are guaranteed to converge when applied to solve (15). For the second issue, we establish an explicit formula in Proposition 2 for computing a valid upper bound of $\Phi^*(\mathcal{F})$ from any inexact primal-dual solution of the SDP problem (15). This result is crucial to allow the use of arbitrary SDP solvers for the computation of the DNN bound, including in particular those solvers with medium accuracy specially designed for large-scale SDPs.

We demonstrate the effectiveness of our approach through extensive computational experiments on both real and synthetic instances. We compare the performance of our algorithms with two of the most powerful commercial solvers `CPLEX` and `Gurobi` and an academic open-source software `quadprogIP` [37]. Our algorithm successfully solves the earlier-mentioned 317,584 instances of dimension $k = 78$ within **3 days** using 32 processors in parallel. For the three instances of dimension $k = 819$, our algorithm is able to solve them in a **few minutes** on a standard laptop. On a set of randomly generated instances of dimension 100 to 500, our algorithm also exhibits superior performance compared with other solvers.

The paper is organized as follows. In Section 2, we study the properties of the DNN relaxation (6), show its connection with the Shor relaxation, and discuss the computation of valid bounds from inexact SDP solutions. In Section 3, we review the cutting plane methods for the reference value problem, propose new cuts based on the DNN relaxation, and show its connection with Konno's cut. In Section 4 we describe our algorithm in detail. We report numerical results in Section 5. In Section 6 we conclude. For clarity of the presentation, some details are moved into the Appendix.

1.5 Notations

Throughout the paper we let $[n] := \{1, \dots, n\}$. We use $\mathbf{0}$ to denote the zero vector or matrix of appropriate dimension, $\mathbf{1}$ to denote the vector of all ones, and \mathbf{I} to denote the identity matrix of appropriate dimension. For any vector $x \in \mathbb{R}^n$ and matrix $X \in \mathbb{R}^{m \times n}$, we use $x_i \in \mathbb{R}$ to denote the i -th entry of x , $X_{i,j} \in \mathbb{R}$ to denote the (i, j) -th entry of X and $X_i \in \mathbb{R}^m$ to denote the i -th column vector of X . We adopt a MATLAB-like notation to represent the submatrix of $X \in \mathbb{R}^{m \times n}$, for example $X_{1:k,n}$ is the submatrix of X formed by the elements at the intersection of the first k rows and the n -th column of X .

For any vector, $x \geq 0$ (resp. $x > 0$) means that x is nonnegative (resp. positive), i.e. all the elements in x are nonnegative (resp. positive). For any two vectors x and y of the same dimension, $x \geq y$ means that $x - y \geq 0$.

For any matrix X , $X \geq 0$ (resp. $X > 0$) means that X is nonnegative (resp. positive), i.e. all the elements in X are nonnegative (resp. positive), and $X \succeq 0$ (resp. $X \succ 0$) means that X is positive semidefinite (resp. positive definite). We denote by \mathcal{S}^n the set of n -by- n symmetric matrices. For two matrices $X, Y \in \mathcal{S}^n$, $X \succeq Y$ means that $X - Y \succeq 0$, and $X \geq Y$ means that $X - Y \geq 0$. We use $\text{diag}(h)$ to represent the diagonal matrix with the diagonal

vector being h . We consider the Frobenius inner product $\langle \cdot, \cdot \rangle$ in the space of matrices, i.e., $\langle A, B \rangle := \text{tr}(A^\top B)$.

2 Doubly Nonnegative Relaxation

The DNN relaxation (6) provides an upper bound for the optimal value of (1). However, it is known from [2, Prop. 8.3] that the feasible region of the SDP problem (6) has no interior. The lack of interior points can be a serious defect from both theoretical and computational aspects. In particular, for problems with no interior feasible point, the strong duality may not hold and convergence of existing SDP solvers is not always guaranteed; see [28] for more discussion.

To resolve this issue, we propose to consider the standard Shor relaxation of the equivalent QCQP problem (see (15) below). We prove the strong duality for the SDP problem obtained from the Shor relaxation and its equivalence with the SDP problem (6) obtained from the DNN relaxation. We also establish a formula for computing a valid upper bound of $\Phi^*(\mathcal{F})$ from an approximate solution returned by any arbitrary SDP solver, which is crucial to adapt the algorithm to a wide range of inexact SDP solvers.

2.1 Equivalence of the DNN relaxation with the Shor relaxation

Adding redundant constraints to (1), we obtain the following equivalent QCQP problem:

$$\begin{aligned} & \max_{y \in \mathbb{R}^k} y^\top Q y + 2d^\top y + \nu \\ & \text{s.t.} \quad F^\top y \leq w \\ & \quad y \geq 0 \\ & \quad (F^\top y - w)(F^\top y - w)^\top \geq 0 \\ & \quad yy^\top \geq 0 \\ & \quad (F^\top y - w)y^\top \leq 0. \end{aligned} \tag{14}$$

It is easy to see that the optimal value of (14) is equal to $\Phi^*(\mathcal{F})$. The standard Shor relaxation of the QCQP problem (14) yields the following SDP problem:

$$\begin{aligned} & \max_{Y \in \mathcal{S}^k, y \in \mathbb{R}^k} \langle Q, Y \rangle + 2d^\top y + \nu \\ & \text{s.t.} \quad F^\top y \leq w \\ & \quad y \geq 0 \\ & \quad F^\top Y F - wy^\top F - F^\top y w^\top + ww^\top \geq 0 \\ & \quad Y \geq 0 \\ & \quad wy^\top - F^\top Y \geq 0 \\ & \quad \begin{pmatrix} Y & y \\ y^\top & 1 \end{pmatrix} \succeq 0. \end{aligned} \tag{15}$$

Remark 1 The proof of Lemma 1 shows how to construct an optimal solution of (15) from an optimal solution of (6), and vice versa.

Remark 2 The size of the largest SDP matrix in (6) is $n + 1$, while the size of the largest SDP matrix in (15) is $k + 1$. This already suggests that (15) could be computationally more favorable than (6). Moreover, we will show in the next subsection that the strong duality holds for (15).

2.2 Strong duality

We consider the SDP relaxation in the form of (15). Let us express (15) in the following abstract way:

$$\begin{aligned} & \max_{\hat{Y} \in \mathcal{S}^{k+1}} \langle \hat{Q}, \hat{Y} \rangle \\ & \text{s.t.} \quad \langle W^{(i,j)}, \hat{Y} \rangle \leq 0, \quad 0 \leq i < j \leq k + m \\ & \quad \langle W^0, \hat{Y} \rangle = 1 \\ & \quad \hat{Y} \succeq 0. \end{aligned} \tag{17}$$

Here,

$$\hat{Q} := \begin{pmatrix} Q & d \\ d^\top & \nu \end{pmatrix}, \quad W^0 := \begin{pmatrix} \mathbf{0} & \mathbf{0} \\ \mathbf{0}^\top & 1 \end{pmatrix},$$

and $\{W^{(i,j)} : 0 \leq i < j \leq k + m\}$ are matrices for representing the polyhedral constraints in (15):

$$W^{(i,j)} := \begin{cases} \begin{pmatrix} \mathbf{0} & -e_j \\ -e_j^\top & 0 \end{pmatrix} & i = 0, \quad 1 \leq j \leq k \\ \begin{pmatrix} \mathbf{0} & F_{j-k} \\ F_{j-k}^\top & -2w_{j-k} \end{pmatrix} & i = 0, \quad k < j \leq k + m \\ \begin{pmatrix} -e_i e_j^\top & -e_j e_i^\top & \mathbf{0} \\ \mathbf{0}^\top & 0 \end{pmatrix} & 1 \leq i < j \leq k \\ \begin{pmatrix} F_{j-k} e_i^\top + e_i F_{j-k}^\top & -w_{j-k} e_i \\ -w_{j-k} e_i^\top & 0 \end{pmatrix} & 1 \leq i \leq k < j \leq m + k \\ \begin{pmatrix} -F_{j-k} F_{i-k}^\top - F_{i-k} F_{j-k}^\top & w_{i-k} F_{j-k} + w_{j-k} F_{i-k} \\ w_{i-k} F_{j-k}^\top + w_{j-k} F_{i-k}^\top & -2w_{i-k} w_{j-k} \end{pmatrix} & k + 1 \leq i < j \leq m + k. \end{cases}$$

Here, e_1, \dots, e_k are the standard basis vectors of \mathbb{R}^k . The dual of (15) can thus be written as:

$$\begin{aligned} & \min \lambda_0 \\ & \text{s.t.} \quad \hat{Q} + \sum_{i < j} \lambda_{i,j} W^{(i,j)} - \lambda_0 W^0 \preceq 0 \\ & \quad \lambda_{i,j} \leq 0, \quad 0 \leq i < j \leq k + m. \end{aligned} \tag{18}$$

Now we establish the strong duality between (17) and its dual (18) under the following assumption.

Assumption 1 \mathcal{F} is bounded and has nonempty interior.

Lemma 2 If \mathcal{F} has nonempty interior, there exists a solution (Y, y) strictly feasible to (15).

Proof Let $y^0 \in \mathbb{R}^k$ such that $F^\top y^0 < w$ and $y^0 > 0$. Let $\epsilon > 0$ and $y^i = y^0 + \epsilon e_i$ for each $i \in [k]$. Choose $\epsilon > 0$ sufficiently small so that $\{y^1, \dots, y^k\}$ are all in the set $\{y \in \mathbb{R}^k : F^\top y \leq w, y \geq 0\}$. Let

$$Y^i = y^i (y^i)^\top, \quad \forall i \in \{0\} \cup [k].$$

Then for each i , (Y^i, y^i) is a feasible solution to (15). Let

$$Y = \frac{1}{k+1} \sum_{i=0}^k Y^i, \quad y = \frac{1}{k+1} \sum_{i=0}^k y^i.$$

Clearly (Y, y) is feasible to (15). Since the vectors $\left\{ \begin{pmatrix} y^0 \\ 1 \end{pmatrix}, \dots, \begin{pmatrix} y^k \\ 1 \end{pmatrix} \right\}$ are linearly independent, the rank of the matrix $\begin{pmatrix} Y & y \\ y^\top & 1 \end{pmatrix}$ is $k+1$. It follows that (Y, y) is strictly feasible to (15). \square

Lemma 3 If \mathcal{F} is bounded and there is at least one $y \in \mathcal{F}$ such that $y > 0$, the dual SDP problem (18) is strictly feasible.

Proof The conditions imply the existence of some $t_* > 0$ such that

$$\begin{aligned} t_* &= \max_{y \in \mathbb{R}^k} \mathbf{1}^\top y \\ \text{s.t.} \quad & F^\top y \leq w \\ & y \geq 0. \end{aligned} \tag{19}$$

By the strong duality of (19), there is $a \in \mathbb{R}_+^m$ such that

$$h := Fa \geq \mathbf{1}, \quad a^\top w = t_*.$$

We have

$$\begin{aligned} & \sum_{i=1}^k \sum_{j=k+1}^{k+m} a_{j-k} W^{(i,j)} \\ &= \sum_{i=1}^k \sum_{j=1}^m a_j \begin{pmatrix} F_j e_i^\top + e_i F_j^\top & -w_j e_i \\ -w_j e_i^\top & 0 \end{pmatrix} \\ &= \sum_{i=1}^k \begin{pmatrix} h e_i^\top + e_i h^\top & -t_* e_i \\ -t_* e_i^\top & 0 \end{pmatrix} \\ &= \begin{pmatrix} h \mathbf{1}^\top + \mathbf{1} h^\top & -t_* \mathbf{1} \\ -t_* \mathbf{1}^\top & 0 \end{pmatrix}. \end{aligned}$$

Thus

$$\begin{aligned}
& \sum_{i=1}^k \sum_{j=k+1}^{k+m} a_{j-k} W^{(i,j)} + \sum_{1 \leq i < j \leq k} (h_i + h_j) W^{(i,j)} \\
&= \begin{pmatrix} h \mathbf{1}^\top + \mathbf{1} h^\top & -t_* \mathbf{1} \\ -t_* \mathbf{1}^\top & 0 \end{pmatrix} + \sum_{1 \leq i < j \leq k} (h_i + h_j) \begin{pmatrix} -e_i e_j^\top & -e_j e_i^\top & \mathbf{0} \\ \mathbf{0}^\top & e_i e_i^\top & 0 \end{pmatrix} \\
&= \begin{pmatrix} 2 \operatorname{diag}(h) & -t_* \mathbf{1} \\ -t_* \mathbf{1}^\top & 0 \end{pmatrix}.
\end{aligned}$$

It follows that

$$\begin{aligned}
& \sum_{i=1}^k \sum_{j=k+1}^{k+m} a_{j-k} W^{(i,j)} + \sum_{1 \leq i < j \leq k} (h_i + h_j) W^{(i,j)} + kt_*^2 W^0 \\
&= \begin{pmatrix} 2 \operatorname{diag}(h) & -t_* \mathbf{1} \\ -t_* \mathbf{1}^\top & kt_*^2 \end{pmatrix}.
\end{aligned}$$

Since

$$(-t_* \mathbf{1})^\top (2 \operatorname{diag}(h))^{-1} (-t_* \mathbf{1}) = \frac{1}{2} t_*^2 \left(\sum_{i=1}^k h_i^{-1} \right) \leq \frac{kt_*^2}{2},$$

and $t_* > 0$, we have

$$\sum_{i=1}^k \sum_{j=k+1}^{k+m} a_{j-k} W^{(i,j)} + \sum_{1 \leq i < j \leq k} (h_i + h_j) W^{(i,j)} + kt_*^2 W^0 \succ 0.$$

Therefore, if we take

$$\begin{aligned}
\lambda_{i,j} &= -\rho a_{j-k}, \quad 1 \leq i \leq k < j \leq k+m, \\
\lambda_{i,j} &= -\rho(h_i + h_j), \quad 1 \leq i < j \leq k, \\
\lambda_0 &= \rho kt_*^2,
\end{aligned}$$

for sufficiently large $\rho > 0$, and take other $\lambda_{i,j}$ (where $i = 0$ or $i > k$) to be 0, we see that there exist $\{\lambda_{i,j} : 0 \leq i < j \leq n\} \subset \mathbb{R}_-$ and $\lambda_0 \in \mathbb{R}$ such that

$$\hat{Q} + \sum_{i < j} \lambda_{i,j} W^{(i,j)} - \lambda_0 W^0 \prec 0.$$

□

By Lemma 2 and 3, we establish Slater's condition and it straightforwardly implies the strong duality for the SDP relaxation (15).

Proposition 1 *Under Assumption 1, both the SDP problem (15) and its dual SDP problem (18) have an optimal solution and the strong duality holds.*

As a result, convergence of state-of-the-art SDP algorithms, such as SDPT3 [32] and SDPNAL+ [30] which require the existence of an interior point in the feasible region, is guaranteed.

2.3 Valid DNN bound from inexact SDP solution

Hereinafter, we will assume that Assumption 1 holds. By Lemma 1, in order to compute the DNN bound $\hat{\Phi}(\mathcal{F})$, we can solve the SDP problem (15). With the strong duality property of (15), we rest assured for the convergence of a wide range of SDP solvers. We mention in particular the interior point type methods and the augmented Lagrangian type methods. There are many powerful commercial and academic solvers that implement these methods: MOSEK, SDPT3 [32], SDPNAL+ [30], etc.

However, it is important to note that any numerical solver using finite floating-point arithmetic is incapable of returning the exact value of $\hat{\Phi}(\mathcal{F})$. Indeed, such numerical solvers terminate when a solution with sufficiently small constraint violation and primal dual optimality gap is found. The value returned by the numerical SDP solver is only an approximation of the true value $\hat{\Phi}(\mathcal{F})$. Additional care needs to be taken in order to get a valid upper bound of $\Phi^*(\mathcal{F})$.

To be more precise, consider applying any suitable SDP numerical solver to the primal SDP problem (17) and its dual SDP problem (18). Let $\epsilon > 0$ and assume that the pair of primal dual solution $(\hat{Y}; \lambda)$ returned by the SDP solver satisfies the following constraint violation and duality gap conditions

$$\begin{cases} \langle W^{(i,j)}, \hat{Y} \rangle \leq \epsilon, & 0 \leq i < j \leq k+m \\ \langle W^0, \hat{Y} \rangle = 1 \\ \hat{Y} \succeq 0 \\ \hat{Q} + \sum_{i < j} \lambda_{i,j} W^{(i,j)} - \lambda_0 W^0 \preceq \epsilon \mathbf{I} \\ \lambda_{i,j} \leq 0, & 0 \leq i < j \leq k+m \\ |\langle \hat{Q}, \hat{Y} \rangle - \lambda_0| \leq \epsilon. \end{cases} \quad (20)$$

As long as $\epsilon > 0$, there is no guarantee that the approximate primal optimal value $\langle \hat{Q}, \hat{Y} \rangle$ or the approximate dual optimal value λ_0 is larger than $\Phi^*(\mathcal{F})$. We next show how to obtain a valid upper bound of $\Phi^*(\mathcal{F})$ from $(\hat{Y}; \lambda)$ satisfying (20).

Lemma 4 *For any feasible solution \hat{Y} of (17), we have*

$$\text{trace}(\hat{Y}) \leq 1 + t_*^2, \quad (21)$$

where $t_* > 0$ is the constant defined in (19).

Proof Let

$$\hat{Y} = \begin{pmatrix} Y & y \\ y^\top & 1 \end{pmatrix}$$

be a feasible solution of (17). In the proof of Lemma 3, we have shown that

$$\sum_{i=1}^k \sum_{j=k+1}^{k+m} a_{j-k} W^{(i,j)} = \begin{pmatrix} h\mathbf{1}^\top + \mathbf{1}h^\top & -t_*\mathbf{1} \\ -t_*\mathbf{1}^\top & 0 \end{pmatrix},$$

where $a_{j-k} \geq 0$ for all $j \in \{k+1, \dots, k+m\}$ and $h \geq \mathbf{1}$. Taking inner product with \hat{Y} on both sides, we obtain

$$\sum_{i=1}^k \sum_{j=k+1}^{k+m} a_{j-k} \langle W^{(i,j)}, \hat{Y} \rangle = \left\langle \begin{pmatrix} h\mathbf{1}^\top + \mathbf{1}h^\top & -t_*\mathbf{1} \\ -t_*\mathbf{1}^\top & 0 \end{pmatrix}, \hat{Y} \right\rangle = 2(h^\top Y \mathbf{1} - t_* \mathbf{1}^\top y).$$

Therefore, since $\langle W^{(i,j)}, \hat{Y} \rangle \leq 0$ and $a_{j-k} \geq 0$, we have

$$h^\top Y \mathbf{1} \leq t_* \mathbf{1}^\top y \leq t_*^2.$$

Since $h \geq \mathbf{1}$, we have $\mathbf{I} \leq \mathbf{1}h^\top$. Finally, since $Y \geq 0$, it follows that

$$\text{trace}(Y) = \langle Y, \mathbf{I} \rangle \leq \langle Y, \mathbf{1}h^\top \rangle = h^\top Y \mathbf{1} \leq t_*^2.$$

□

Proposition 2 *Let $\epsilon > 0$ and let $(\hat{Y}; \lambda)$ be a pair of approximate primal and dual solutions satisfying the gap conditions in (20). Then,*

$$\bar{\Phi}(\mathcal{F}) \leq \epsilon(t_*^2 + 1) + \lambda_0. \quad (22)$$

Proof Let (\hat{Y}^*, λ^*) be an optimal primal dual solution pair. Then,

$$\begin{aligned} \bar{\Phi}(\mathcal{F}) &= \langle \hat{Q}, \hat{Y}^* \rangle \\ &= \langle \hat{Q} + \sum_{i < j} \lambda_{i,j} W^{(i,j)} - \lambda_0 W^0, \hat{Y}^* \rangle - \sum_{i < j} \lambda_{i,j} \langle W^{(i,j)}, \hat{Y}^* \rangle + \lambda_0 \langle W^0, \hat{Y}^* \rangle \\ &\stackrel{(20)}{\leq} \epsilon \text{trace}(\hat{Y}^*) + \lambda_0 \\ &\stackrel{(21)}{\leq} \epsilon(1 + t_*^2) + \lambda_0. \end{aligned}$$

Here the first equality follows from the fact that $\bar{\Phi}(\mathcal{F})$ is the optimal value of (17). The second equality can be verified directly. The third inequality follows from the conditions in (20) and the positive semidefiniteness of \hat{Y}^* . The last inequality follows from (21). □

Proposition 2 enables us to obtain a valid upper bound of $\Phi^*(\mathcal{F})$ from any approximate primal-dual solution $(\hat{Y}; \lambda)$ returned by any SDP solver. The correction term to be added is $\epsilon(t_*^2 + 1)$, where ϵ depends on the constraint violation and the duality gap, and t_* is defined in (19).

Remark 3 Note that the exact value of t_* , which is the optimal value of the LP problem (19), may not be computable (due to numerical tolerances and finite machine precision). However, formula (22) remains valid if one replaces t_* by any number larger than it. An explicit upper bound is readily available if

F has at least one column with positive elements only. Indeed, if $F_{1,1}, \dots, F_{k,1}$ are all positive, then

$$\begin{aligned} t_* &\leq \max_{y \in \mathbb{R}^k} \mathbf{1}^\top y \\ \text{s.t. } &F_{1,1}y_1 + \dots + F_{k,1}y_k \leq w_1 \\ &y_1, \dots, y_k \geq 0. \end{aligned}$$

The optimal value of the above LP problem is known to be $w_1 (\min(F_{1,1}, \dots, F_{k,1}))^{-1}$.

2.4 Upper bound of the DNN bound

In this subsection, we establish an upper bound for the DNN bound $\bar{\Phi}(\mathcal{F})$. This result will be useful in the later section when we compare different cuts.

Proposition 3 *Let $\Lambda \in \mathbb{R}_+^{k \times m}$ and $P \in \mathbb{R}_+^{k \times k} \cap \mathcal{S}^k$ be nonnegative matrices such that*

$$-Q - P + \Lambda F^\top + F \Lambda^\top \succeq 0. \quad (23)$$

Then,

$$\bar{\Phi}(\mathcal{F}) \leq \nu + \max \left\{ 2(d + \Lambda w)^\top y : F^\top y \leq w, y \geq 0 \right\}.$$

Proof Let (Y, y) be a feasible solution of (15). Since $P \geq 0$ and $Y \geq 0$, we have

$$\langle -P, Y \rangle \leq 0. \quad (24)$$

Since

$$\Lambda \geq 0, \quad w y^\top - F^\top Y \geq 0, \quad (25)$$

we have

$$\langle \Lambda F^\top + F \Lambda^\top, Y \rangle = 2\langle \Lambda, F^\top Y \rangle \leq 2\langle \Lambda, w y^\top \rangle = 2(d + \Lambda w)^\top y. \quad (26)$$

Here, the inequality follows from (25). Hence,

$$\begin{aligned} \langle Q, Y \rangle + 2d^\top y &\leq \langle -P + \Lambda F^\top + F \Lambda^\top, Y \rangle + 2d^\top y \\ &\leq 2(d + \Lambda w)^\top y. \end{aligned} \quad (27)$$

Here, the first inequality follows from (23) and the fact that $Y \succeq 0$, and the second inequality follows from (24) and (26). If (Y^*, y^*) is an optimal solution of (6) (the existence follows from Proposition 1), then

$$\begin{aligned} \bar{\Phi}(\mathcal{F}) &= \langle Q, Y^* \rangle + 2d^\top y^* + \nu \\ &\leq \nu + 2(d + \Lambda w)^\top y^* \\ &\leq \nu + \max \left\{ 2(d + \Lambda w)^\top y : F^\top y \leq w, y \geq 0 \right\}. \end{aligned}$$

Here, the first inequality follows from (27), and the second inequality uses the fact that y^* satisfies $F^\top y^* \leq w$ and $y^* \geq 0$. \square

3 Generation of Valid Cuts

In this section we review the idea of cutting plane algorithms and present classical as well as novel methods for the generation of valid cuts at any given KKT vertex.

Recall that we have, at our disposal, a reference value ν_R and the task is to determine whether

$$\nu_R > \Phi^*(\mathcal{F}) \quad \text{or} \quad \Phi^*(\mathcal{F}) \geq \nu_R ? \quad (28)$$

For ease of presentation, we assume without loss of generality that the KKT vertex of interest is the origin point $\mathbf{0} \in \mathbb{R}^k$ and the following three conditions hold:

$$w \geq 0, \quad (29a)$$

$$d \leq 0, \quad (29b)$$

$$\nu < \nu_R. \quad (29c)$$

The first condition implies that $\mathbf{0}$ is a vertex. The second condition implies that $\mathbf{0}$ is a KKT point. The third condition means that the objective value at $\mathbf{0}$ is strictly smaller than the reference value ν_R . For details on reducing the general case to the case satisfying (29), see Appendix B.

3.1 Cutting plane method

Under the three conditions in (29), in order to generate a valid cutting plane at the origin point $\mathbf{0} \in \mathbb{R}^k$, we search for a nonnegative vector $\theta \in \mathbb{R}_+^k$ such that

$$\begin{aligned} \nu_R &> \max_{y \in \mathbb{R}^k} y^T Q y + 2d^T y + \nu \\ \text{s.t.} \quad &F^T y \leq w \\ &y \geq 0 \\ &\theta^T y \leq 1. \end{aligned} \quad (30)$$

If (30) holds, then the cut $\{y \in \mathbb{R}^k : \theta^T y \geq 1\}$ is said to be *valid* and

$$\Phi^*(\mathcal{F}_\theta) \leq \Phi^*(\mathcal{F}) \leq \max(\nu_R, \Phi^*(\mathcal{F}_\theta)),$$

where \mathcal{F}_θ is defined as the intersection of the original feasible region \mathcal{F} and the cut $\{y \in \mathbb{R}^k : \theta^T y \geq 1\}$:

$$\mathcal{F}_\theta := \mathcal{F} \cap \{y \in \mathbb{R}^k : \theta^T y \geq 1\}.$$

It is important to note that $\mathbf{0} \notin \mathcal{F}_\theta$ and hence \mathcal{F}_θ is strictly included in \mathcal{F} . In order to determine (28), it suffices to determine whether

$$\nu_R > \Phi^*(\mathcal{F}_\theta) \quad \text{or} \quad \Phi^*(\mathcal{F}_\theta) \geq \nu_R ? \quad (31)$$

Thus the problem is reduced with a strictly smaller feasible region \mathcal{F}_θ . Repeating this procedure of adding valid cuts, the feasible region is reduced at each iteration until we find an answer to (31).

In the following, we present different methods to find a nonnegative vector θ satisfying (30).

3.2 Tuy's and Konno's cut revisited

We give a brief review of Tuy and Konno's work [17,18,33]. For ease of discussion, we denote for any $\theta \in \mathbb{R}_+^k$ that

$$\Delta(\theta) := \left\{ y \in \mathbb{R}^k : \sum_{i=1}^k y_i \theta_i \leq 1, y \geq 0 \right\}.$$

We start with a basic result which is essential in both Tuy and Konno's argument.

Lemma 5 *Let $f : \mathbb{R}^k \rightarrow \mathbb{R}$ be a convex function and $\theta > 0$. Then,*

$$\max \{f(y) : y \in \Delta(\theta)\} = \max \{f(\mathbf{0}), f(\theta_1^{-1}e_1), \dots, f(\theta_k^{-1}e_k)\}.$$

Proof When $\theta > 0$, $\Delta(\theta)$ is a simplex with vertices $\{\mathbf{0}, \theta_1^{-1}e_1, \dots, \theta_k^{-1}e_k\}$. The statement follows from the fact that the maximum value of f is attained at one vertex of $\Delta(\theta)$. \square

When $\theta \geq 0$ contains zero elements, $\Delta(\theta)$ is not a simplex and it is not enough to directly examine the function value at the vertices of $\Delta(\theta)$. To handle this issue, we present below a generalization of Lemma 5 which covers all the cases of $\theta \geq 0$.

Lemma 6 *Let $f : \mathbb{R}^k \rightarrow \mathbb{R}$ be a convex function and $\gamma \geq f(\mathbf{0})$. Assume that for any $i \in [k]$, there is $\eta > 0$ such that $f(\eta^{-1}e_i) \leq \gamma$. Define the vector $\theta \in \mathbb{R}_+^k$ as follows:*

$$\theta_i := \inf\{\eta > 0 : f(\eta^{-1}e_i) \leq \gamma\}, \quad i = 1, \dots, k.$$

Then

$$\max \{f(y) : y \in \Delta(\theta)\} \leq \gamma.$$

Proof Let $\rho > 0$. For each $i \in [k]$, if $f(\rho^{-1}e_i) > \gamma$, then $f(\eta^{-1}e_i) > \gamma$ for any $0 < \eta \leq \rho$. This follows from the convexity of f and $f(\mathbf{0}) \leq \gamma$. Hence for any $\rho > \theta_i$ we must have $f(\rho^{-1}e_i) \leq \gamma$.

Fix any $y \in \Delta(\theta)$. For any $t \geq \max((\sum_{i=1}^k y_i)^2, 1)$, we have $\theta + \frac{1}{t}\mathbf{1} > \mathbf{0}$ and

$$\begin{aligned} & \sum_{i=1}^k \left(\theta_i + \frac{1}{t} \right) \left(1 - \frac{1}{\sqrt{t}} \right) y_i \\ &= \left(1 - \frac{1}{\sqrt{t}} \right) \left(\sum_{i=1}^k \theta_i y_i + \frac{1}{t} \sum_{i=1}^k y_i \right) \\ &\leq \left(1 - \frac{1}{\sqrt{t}} \right) \left(1 + \frac{1}{t} \sum_{i=1}^k y_i \right) \\ &\leq \left(1 - \frac{1}{\sqrt{t}} \right) \left(1 + \frac{1}{\sqrt{t}} \right) \leq 1, \end{aligned}$$

hence $\left(1 - \frac{1}{\sqrt{t}} \right) y \in \Delta\left(\theta + \frac{1}{t}\mathbf{1}\right)$. By Lemma 5 we know that for sufficiently large $t > 0$:

$$f\left(\left(1 - \frac{1}{\sqrt{t}}\right)y\right) \leq \max\left(f(\mathbf{0}), \max_{i=1, \dots, k} f\left(\frac{t}{t\theta_i + 1} e_i\right)\right) \leq \gamma.$$

Hence, $f(y) \leq \gamma$ by the continuity of f . \square

Tuy [33] proposed to use the following value

$$\max\{\Phi(y) : y \in \Delta(\theta)\} \quad (32)$$

as an upper bound of $\max\{\Phi(y) : y \in \mathcal{F} \cap \Delta(\theta)\}$. Let $0 < \delta < \nu_R - \nu$ and define

$$\tau_i := \inf\{\eta > 0 : \Phi(\eta^{-1} e_i) \leq \nu_R - \delta\}, \quad i = 1, \dots, k. \quad (33)$$

It can be checked that

$$\tau_i = \frac{Q_{ii}}{-d_i + \sqrt{d_i^2 + Q_{ii}(\nu_R - \delta - \nu)}}, \quad i = 1, \dots, k. \quad (34)$$

Note that τ_i in (34) is well-defined for any $\delta < \nu_R - \nu$. If $Q_{ii} = 0$ for some i , then $\tau_i = 0$. Applying Lemma 6 with $f = \Phi$ and $\gamma = \nu_R - \delta$, we obtain

$$\max\{\Phi(y) : y \in \mathcal{F} \cap \Delta(\tau)\} \leq \max\{\Phi(y) : y \in \Delta(\tau)\} \leq \nu_R - \delta.$$

Thus the cut $\{y \in \mathbb{R}^k : \tau^\top y \geq 1\}$ is a valid cut, known as Tuy's cut.

Next we recall the method proposed by Konno in [17], for improving any valid cut including in particular Tuy's cut. Given Tuy's cut τ defined in (34), we next deal with the following program:

$$\begin{aligned} \phi_{\tau, \theta}^* &:= \max_{y \in \mathbb{R}^k} y^\top Q y + 2d^\top y + \nu \\ \text{s.t.} \quad & F^\top y \leq w \\ & y \geq 0 \\ & \tau^\top y \geq 1 \\ & \theta^\top y \leq 1. \end{aligned} \quad (35)$$

Recall that \mathcal{F}_τ is the reduced region

$$\mathcal{F}_\tau = \mathcal{F} \cap \{y \in \mathbb{R}^k : \tau^\top y \geq 1\},$$

which is assumed to be nonempty (otherwise the reference value problem is solved). Konno [17] proposed to use

$$\bar{\phi}_{\tau,\theta}^K := \max \{\tilde{y}^\top Qy + d^\top \tilde{y} + d^\top y + \nu : y \in \Delta(\theta), \tilde{y} \in \mathcal{F}_\tau\} \quad (36)$$

as an upper bound of $\phi_{\tau,\theta}^*$. The key observation made by Konno is that,

$$\bar{\phi}_{\tau,\theta}^K = \max \{g(y) : y \in \Delta(\theta)\}, \quad (37)$$

where $g : \mathbb{R}^k \rightarrow \mathbb{R}$ is a convex function defined by:

$$g(y) := \max \{\tilde{y}^\top Qy + d^\top \tilde{y} + d^\top y + \nu : \tilde{y} \in \mathcal{F}_\tau\}.$$

Next, we define the vector θ_K which formulates Konno's cut. The entries of θ_K for a given $0 < \delta' < \nu_R - \nu$ are defined as²:

$$(\theta_K)_i := \inf \{\eta > 0 : g(\eta^{-1}e_i) \leq \nu_R - \delta'\}, \quad \forall i = 1, \dots, k. \quad (38)$$

Again, applying Lemma 6 with $f = g$ and $\gamma = \nu_R - \delta'$, together with (37) we obtain

$$\phi_{\tau,\theta}^* \leq \bar{\phi}_{\tau,\theta_K}^K \leq \nu_R - \delta' < \nu_R. \quad (39)$$

The cut $\{y \in \mathbb{R}^k : \theta_K^\top y \geq 1\}$ is a valid cut, which we will refer to as Konno's cut.

Remark 4 Konno [18, Thm 3.3] showed that the computation of each $(\theta_K)_i$ can be done by solving an LP program; see Appendix D for details.

We next present a lemma which allows us to argue that Konno's cut is generally deeper than Tuy's cut for a particular choice of δ' .

Lemma 7 *Without loss of generality, suppose that $\tau_1 = \dots = \tau_\ell = 0$ and $\tau_{\ell+1} > 0, \dots, \tau_k > 0$ for some $\ell \in \{0, \dots, k\}$. Define:*

$$y^i \in \arg \max \{(\tau_i^{-1}Q_i + d)^\top y : y \in \mathcal{F}_\tau\}, \quad i = \ell + 1, \dots, k,$$

and

$$\omega = \max \{\Phi(y^i) : i = \ell + 1, \dots, k\}. \quad (40)$$

Then

$$(\theta_K)_i = 0, \quad i = 1, \dots, \ell, \quad (41)$$

and

$$g(\tau_i^{-1}e_i) \leq \frac{\nu_R + \omega}{2}, \quad i = \ell + 1, \dots, k. \quad (42)$$

² The perturbation parameter δ' here may be different from the parameter δ used in Tuy's cut (33).

We defer the proof to Appendix C. Let us elaborate on the utilization of Lemma 7. If $\omega \geq \nu_R$, then the reference value problem (28) is solved. Otherwise, as long as

$$\delta' \leq \frac{\nu_R - \omega}{2}, \quad (43)$$

we know from Lemma 7 that

$$g(\tau_i^{-1}e_i) \leq \nu_R - \frac{\nu_R - \omega}{2} \leq \nu_R - \delta', \quad \forall i = \ell + 1, \dots, k.$$

Then from Equation (38) we deduce that $\theta_K \leq \tau$, i.e., Konno's cut is deeper than Tuy's cut.

In the remaining of this section, we will present a new method to further improve Konno's cut. Recall that the key idea in generating Konno's cut is to give a computable upper bound on $\phi_{\tau, \theta}^*$ defined in (35). For finding deeper cuts, we next propose two computable upper bounds of $\phi_{\tau, \theta}^*$ which are tighter than Konno's bound $\bar{\phi}_{\tau, \theta}^K$ defined in (36).

3.3 Tighter bound from the LP relaxation

We start with an estimate of $\bar{\phi}_{\tau, \theta}^K$ for any positive vector θ .

Lemma 8 *For any $\theta > 0$ we have*

$$\begin{aligned} \bar{\phi}_{\tau, \theta}^K &\geq \min \quad \beta + \nu \\ \text{s.t.} \quad &Q \leq -\Lambda_0 \tau^\top - \tau \Lambda_0^\top + \Lambda F^\top + F \Lambda^\top - \frac{1}{2} (d\theta^\top + \theta d^\top) \\ &d \leq \beta \theta + 2\Lambda_0 - 2\Lambda w \\ &\Lambda_0 \geq 0, \Lambda \geq 0. \end{aligned} \quad (44)$$

Proof Let $\beta = \bar{\phi}_{\tau, \theta}^K - \nu$. In view of (37),

$$g(\theta_i^{-1}e_i) - \nu = \max_{y \in \mathcal{F}_\tau} (\theta_i^{-1}Q_i + d)^\top y + \theta_i^{-1}d_i \leq \beta, \quad \forall i \in [k].$$

Consequently, for each $i \in [k]$, the following system (on $y \in \mathbb{R}^k$) is infeasible:

$$\begin{cases} (\theta_i^{-1}Q_i + d)^\top y > \beta - \theta_i^{-1}d_i \\ \tau^\top y \geq 1 \\ F^\top y \leq w \\ y \geq 0 \end{cases} \quad (45)$$

By Farkas' Lemma and $\mathcal{F}_\tau \neq \emptyset$, for each $i \in [k]$, the infeasibility of (45) implies the feasibility of the following system (on $u_0^i \in \mathbb{R}$ and $u^i \in \mathbb{R}^m$):

$$\begin{cases} \theta_i^{-1}Q_i + d \leq -u_0^i \tau + F u^i \\ \beta - \theta_i^{-1}d_i \geq -u_0^i + (u^i)^\top w \\ u_0^i \geq 0, u^i \geq 0 \end{cases} \quad (46)$$

Multiplying both sides of the inequalities by the positive number θ_i , the system (46) can be equivalently written as

$$\begin{cases} Q_i + \theta_i d \leq -u_0^i \tau + F u^i \\ \beta \theta_i - d_i \geq -u_0^i + (u^i)^\top w \\ u_0^i \geq 0, u^i \geq 0 \end{cases} \quad (47)$$

The fact that the system (47) is solvable for each $i \in [k]$ implies that the following system on $(\Lambda_0 \in \mathbb{R}^k, \Lambda \in \mathbb{R}^{k \times m})$ is solvable:

$$\begin{cases} Q \leq -\Lambda_0 \tau^\top - \tau \Lambda_0^\top + \Lambda F^\top + F \Lambda^\top - \frac{1}{2} (d \theta^\top + \theta d^\top) \\ d \leq \beta \theta + 2\Lambda_0 - 2\Lambda w \\ \Lambda_0 \geq 0, \Lambda \geq 0 \end{cases} \quad (48)$$

To see this, just let $\Lambda_0 = \frac{1}{2} (u_0^1 \cdots u_0^k)^\top$ and $\Lambda = \frac{1}{2} (u^1 \cdots u^k)^\top$ and use the fact that $Q = Q^\top$. \square

Remark 5 In general the inequality in (44) is strict since (48) cannot imply (47).

We next show that the lower bound of $\bar{\phi}_{\tau, \theta}^K$ provided by Lemma 8 is also an upper bound of $\phi_{\tau, \theta}^*$. For this, consider the following extended LP program:

$$\begin{aligned} \bar{\phi}_{\tau, \theta}^L := \min \quad & -\alpha + q^\top w + \beta + \nu \\ \text{s.t.} \quad & Q \leq -\Lambda_0 \tau^\top - \tau \Lambda_0^\top + \Lambda F^\top + F \Lambda^\top + (\Lambda_{m+1} \theta^\top + \theta \Lambda_{m+1}^\top) \\ & 2d - 2\Lambda_0 + 2\Lambda w + 2\Lambda_{m+1} \leq -\alpha \tau + Fq + \beta \theta \\ & \Lambda_0 \geq 0, \Lambda \geq 0, \Lambda_{m+1} \geq 0, \alpha \geq 0, q \geq 0, \beta \geq 0. \end{aligned} \quad (49)$$

Proposition 4 For any positive vector $\theta \in \mathbb{R}^k$, we have

$$\bar{\phi}_{\tau, \theta}^K \geq \bar{\phi}_{\tau, \theta}^L \geq \phi_{\tau, \theta}^*. \quad (50)$$

Proof Any feasible solution to the optimization problem in (44) can be extended to a feasible solution of (49) by letting

$$\alpha = 0, \quad q = \mathbf{0}, \quad \Lambda_{m+1} = -d/2.$$

(Recall that $d \leq 0$.) Then we apply Lemma 8 to obtain the first inequality.

Let $\Lambda_0, \Lambda, \Lambda_{m+1}, \alpha, q, \beta$ be feasible to (49). Then for any $y \in \mathcal{F}_\tau \cap \Delta(\theta)$, we have

$$\begin{aligned} y^\top Q y &\leq -2y^\top \tau \Lambda_0^\top y + 2y^\top \Lambda F^\top y + 2y^\top \Lambda_{m+1} \theta^\top y \\ &\leq -2\Lambda_0^\top y + 2y^\top \Lambda w + 2y^\top \Lambda_{m+1}. \end{aligned}$$

Here, the first inequality follows from the first constraint of (49) and $y \geq 0$. The second inequality follows from the nonnegativity of $\Lambda_0^\top y$, $\Lambda^\top y$ and $\Lambda_{m+1}^\top y$.

and the fact that $\theta^\top y \leq 1$, $\tau^\top y \geq 1$ and $F^\top y \leq w$. Now we use the second constraint of (49) to obtain

$$\begin{aligned} y^\top Qy &\leq -2d^\top y - \alpha\tau^\top y + q^\top F^\top y + \beta\theta^\top y \\ &\leq -2d^\top y - \alpha + q^\top w + \beta. \end{aligned}$$

Hence

$$y^\top Qy + 2d^\top y + \nu \leq -\alpha + q^\top w + \beta + \nu, \quad \forall y \in \mathcal{F}_\tau \cap \Delta(\theta),$$

which implies $\phi_{\tau,\theta}^* \leq \bar{\phi}_{\tau,\theta}^L$. \square

Based on Proposition 4, the vector θ such that $\bar{\phi}_{\tau,\theta}^L = \nu_R - \delta'$ leads to a cut deeper than Konno's cut. Unfortunately, the search of such θ cannot be done by solving k LP programs as for the search of θ_K . Nevertheless, we can try to improve Konno's cut through the standard bisection trick. Specifically, let θ_K be the vector generating Konno's cut and choose some $\theta < \theta_K$. If $\bar{\phi}_{\tau,\theta}^L \leq \nu_R - \delta'$, then we get an improved cut. Otherwise, we increase θ , for example to $(\theta + \theta_K)/2$, and repeat until we get an improved cut.

3.4 Deeper cut by the doubly nonnegative relaxation

In this subsection, we show that a deeper cut than Konno's cut can be achieved by the DNN relaxation. The main results are summarized in Theorem 2.

We begin by rewriting (35) into the form of (1). Let $\hat{F} = (F \theta - \tau)$ and

$\hat{w} = \begin{pmatrix} w \\ 1 \\ -1 \end{pmatrix}$ so that (35) is written as

$$\begin{aligned} \phi_{\tau,\theta}^* &= \max y^\top Qy + 2d^\top y + \nu \\ \text{s.t. } &\hat{F}^\top y \leq \hat{w} \\ &y \geq 0. \end{aligned} \quad (51)$$

Now (51) takes the same form as (1), thus all the results on the DNN relaxation of (1) presented in Section 2 can be directly adapted to the DNN relaxation of (51). Denote by $\bar{\phi}_{\tau,\theta}^D$ the DNN relaxation value of (51), i.e.,

$$\begin{aligned} \bar{\phi}_{\tau,\theta}^D &:= \max_{\substack{Y \in \mathcal{S}^k \\ y \in \mathbb{R}^k}} \langle Q, Y \rangle + 2d^\top y + \nu \\ \text{s.t. } &\hat{F}^\top y \leq \hat{w} \\ &y \geq 0 \\ &\hat{F}^\top Y \hat{F} - \hat{w}y^\top \hat{F} - \hat{F}^\top y\hat{w}^\top + \hat{w}\hat{w}^\top \geq 0 \\ &Y \geq 0 \\ &\hat{w}y^\top - \hat{F}^\top Y \geq 0 \\ &\begin{pmatrix} Y & y \\ y^\top & 1 \end{pmatrix} \succeq 0. \end{aligned} \quad (52)$$

Note that $\bar{\phi}_{\tau,\theta}^D = \bar{\Phi}(\mathcal{F}_\tau \cap \Delta(\theta))$. Using directly Proposition 3 we get the following upper bound of $\bar{\phi}_{\tau,\theta}^D$.

Corollary 1 *If there exists $\Lambda_0, \Lambda_{m+1} \in \mathbb{R}_+^k$, $\Lambda \in \mathbb{R}_+^{k \times m}$ and $P \in \mathbb{R}_+^{k \times k} \cap \mathcal{S}^k$ such that*

$$-Q - P - \Lambda_0 \tau^\top - \tau \Lambda_0^\top + \Lambda F^\top + F \Lambda^\top + \Lambda_{m+1} \theta^\top + \theta \Lambda_{m+1}^\top \succeq 0. \quad (53)$$

Then

$$\bar{\phi}_{\tau,\theta}^D \leq \nu + 2 \max_{y \in \mathcal{F}_\tau \cap \Delta(\theta)} (d - \Lambda_0 + \Lambda w + \Lambda_{m+1})^\top y.$$

Proof Let $\hat{\Lambda} = [\Lambda \ \Lambda_{m+1} \ \Lambda_0] \geq 0$. Then (53) can be written as

$$-Q - P + \hat{\Lambda} \hat{F}^\top + \hat{F} \hat{\Lambda}^\top \succeq 0.$$

Applying Proposition 3, we know that

$$\begin{aligned} \bar{\phi}_{\tau,\theta}^D &\leq \nu + 2 \max \left\{ (d + \hat{\Lambda} \hat{w})^\top y : \hat{F}^\top y \leq \hat{w}, y \geq 0 \right\} \\ &= \nu + 2 \max_{y \in \mathcal{F}_\tau \cap \Delta(\theta)} (d - \Lambda_0 + \Lambda w + \Lambda_{m+1})^\top y. \end{aligned}$$

□

Theorem 2 *For any positive vector $\theta \in \mathbb{R}_{++}^k$, we have*

$$\bar{\phi}_{\tau,\theta}^K \geq \bar{\phi}_{\tau,\theta}^L \geq \bar{\phi}_{\tau,\theta}^D \geq \phi_{\tau,\theta}^*. \quad (54)$$

Proof The first inequality follows from Proposition 4. Let $\Lambda_0, \Lambda, \Lambda_{m+1}, q, \alpha, \beta$ be feasible to the program (49). Let

$$P := -Q - \Lambda_0 \tau^\top - \tau \Lambda_0^\top + \Lambda F^\top + F \Lambda^\top + \Lambda_{m+1} \theta^\top + \theta \Lambda_{m+1}^\top.$$

Then (53) holds trivially. Further, by the first inequality constraint in (49), $P \geq 0$. Corollary 1 allows to deduce:

$$\bar{\phi}_{\tau,\theta}^D \leq \nu + 2 \max_{y \in \mathcal{F}_\tau \cap \Delta(\theta)} (d - \Lambda_0 + \Lambda w + \Lambda_{m+1})^\top y.$$

Now we use the second constraint of (49) to obtain

$$\begin{aligned} &2 \max_{y \in \mathcal{F}_\tau \cap \Delta(\theta)} (d - \Lambda_0 + \Lambda w + \Lambda_{m+1})^\top y \\ &\leq \max_{y \in \mathcal{F}_\tau \cap \Delta(\theta)} (-\alpha \tau + F q + \beta \theta)^\top y \\ &\leq -\alpha + q^\top w + \beta. \end{aligned}$$

Here, the first inequality follows from the second constraint of (49), and the second inequality follows from $\tau^\top y \geq 1$, $F^\top y \leq w$ and $\theta^\top y \leq 1$ for any $y \in \mathcal{F}_\tau \cap \Delta(\theta)$. It follows that

$$\bar{\phi}_{\tau,\theta}^L \geq \bar{\phi}_{\tau,\theta}^D.$$

□

Theorem 2 provides a foundation of the new cutting plane method that we are about to propose. In order to search for a vector θ such that (35) holds, we choose a perturbation parameter $0 < \delta < \nu_R - \nu$ and start by computing the vector τ defined in (34). Then we compute ω defined by (40). If $\omega \geq \nu_R$, the reference value problem is solved. Otherwise we choose $0 < \delta' \leq \frac{\nu_R - \max(\omega, \nu)}{2}$ and compute θ_K defined through (38) such that

$$\bar{\phi}_{\tau, \theta_K}^K \leq \nu_R - \delta'.$$

Then we choose a factor $\eta \in (0, 1)$ and test whether $\theta = \eta\theta_K$ satisfies

$$\bar{\phi}_{\tau, \theta}^L \leq \nu_R - \delta'. \quad (55)$$

If (55) holds, then θ yields a valid cut, which is deeper than Konno's cut. Otherwise we further check if

$$\bar{\phi}_{\tau, \theta}^D \leq \nu_R - \delta'. \quad (56)$$

If (56) holds, then θ yields a valid cut, which is deeper than Konno's cut. The pseudo code of this process is given in Algorithm 6. One can also use the bisection trick mentioned in the end of Section 3.3. In any case, the core theory behind is Theorem 2, which guarantees that

$$\bar{\phi}_{\tau, \theta_K}^D \leq \bar{\phi}_{\tau, \theta_K}^L \leq \bar{\phi}_{\tau, \theta_K}^K \leq \nu_R - \delta' < \nu_R,$$

and provides a way to improve Konno's cut.

4 Algorithm

In this section we summarize our method in Algorithm 1 and Algorithm 2. For the future reference, we name our algorithm as **QuadProgCD**, where the letter "C" refers to the cutting plane method and the letter "D" refers to the doubly nonnegative relaxation.

The algorithm has two variants: 1. **QuadProgCD-R** (Algorithm 1) is designed for solving the reference value problem (28), where we use the suffix **-R** to refer to the reference value problem; 2. **QuadProgCD-G** (Algorithm 2) is designed for solving the global optimization problem (1), where the suffix **-G** refers to the global optimization mode.

4.1 Algorithm for the reference value problem

Algorithm 1 takes as input the positive semidefinite matrix $Q \in \mathcal{S}^k$, the vector $d \in \mathbb{R}^k$ and the scalar $\nu \in \mathbb{R}$ which define the quadratic objective function Φ , the matrix $F \in \mathbb{R}^{k \times m}$ and the vector $w \in \mathbb{R}^m$ which define the feasible region \mathcal{F} , the reference value ν_R , a factor $\eta \in (0, 1)$, and a perturbation parameter $\delta > 0$. The algorithm solves the reference value problem (28) by returning a lower bound $\underline{\nu}$ of $\Phi^*(\mathcal{F})$ and an upper bound $\bar{\nu}$ of $\Phi^*(\mathcal{F})$ such that $\nu_R \notin (\underline{\nu}, \bar{\nu}]$.

Algorithm 1 starts by searching for a KKT vertex \bar{y} of (1) (line 3). There are many ways to achieve a KKT vertex and we adopt the mountain climbing algorithm proposed by Konno in [18]. The details are recalled in Appendix A.

If $\Phi(\bar{y})$ is larger than or equal to ν_R , then we obtain a lower bound \underline{v} such that $\nu_R \leq \underline{v} \leq \Phi^*(\mathcal{F})$. Otherwise, we compute the DNN bound $\bar{\Phi}(\mathcal{F})$. If the latter is strictly smaller than ν_R , then we obtain an upper bound \bar{v} such that $\nu_R > \bar{v}$ (note that if $\mathcal{F} = \emptyset$, we would also reach this case because $\bar{\Phi}(\mathcal{F}) = -\infty$). Otherwise, we proceed to the cutting plane step (from line 13 to line 31).

In line 13 we make a suitable change of coordinate so that \bar{y} is transformed to the origin point $\mathbf{0}$ and compute the parameters (Q, d, ν, F, w) under the new basis. For details of this step please check Appendix B. In line 14 we make sure that δ is smaller than $\nu_R - \nu$. In line 16 we compute the vector τ which defines Tuy's cut. From line 18 to line 26 we check whether ω defined in (40) is larger than ν_R . If yes, then we obtain a lower bound \underline{v} such that $\nu_R \leq \underline{v} \leq \Phi^*(\mathcal{F})$. Otherwise, we update δ so that it does not increase and satisfies (43) in line 27. Then we proceed to generate a deeper cut (from line 28 to line 31).

We provide two options for the generation of a cut deeper than Tuy's cut. The first option is to use Konno's cut as recalled in Section 3.2. The second option is to generate an even deeper cut using the theory that we developed in Section 3.4. The two algorithms for option I and II are described in Appendix D and Appendix E.

In the while loop, the lower bound \underline{v} is nondecreasing and the upper bound \bar{v} is nonincreasing. When we solve the reference value problem (28), the while loop breaks when either $\nu_R \leq \underline{v}$ or $\nu_R > \bar{v}$ so that the reference value problem is solved.

4.2 Algorithm for global solution of the concave QP problem

Now we present **QuadProgCD-G** as in Algorithm 2 for globally solving the concave QP problem (1). **QuadProgCD-G** follows a similar structure as Algorithm 1, with some differences that we detail below.

The input of Algorithm 2 includes a gap tolerance $\epsilon > 0$. The output is a lower bound \underline{v} and an upper bound \bar{v} of $\Phi^*(\mathcal{F})$ such that

$$\frac{\bar{v} - \underline{v}}{\max\{\epsilon, |\underline{v}|\}} \leq \epsilon. \quad (57)$$

Here, we take the maximum of ϵ and $|\underline{v}|$ in the denominator to handle the pathological case $|\underline{v}| = 0$.

There is no longer a prescribed reference value ν_R . Instead, Algorithm 2 uses a dynamic reference value, which is set to be the lower bound $\underline{v} + \epsilon^2$ and updated throughout the iterations (lines 4 and 17). The termination criteria are also modified to ensure global convergence (lines 2, 7 and 18).

Another difference with Algorithm 1 is that in Algorithm 2 the perturbation parameter δ is set to be zero. This is because Algorithm 2 uses the

Algorithm 1 QuadProgCD-R

Input: $Q \succeq 0$, $d \in \mathbb{R}^k$, $\nu \in \mathbb{R}$, $F \in \mathbb{R}^{k \times m}$, $w \in \mathbb{R}^m$, reference value $\nu_R \in \mathbb{R}$, factor $\eta \in (0, 1)$, perturbation $\delta > 0$.

- 1: $\underline{v} \leftarrow -\infty, \bar{v} \leftarrow \infty$;
- 2: **while** $\underline{v} < \nu_R \leq \bar{v}$ **do**
- 3: $\bar{y} \leftarrow \text{Search_of_KKT_Point}(Q, d, \nu, F, w)$; \triangleright See Algorithm 3.
- 4: **if** $\bar{y}^\top Q \bar{y} + 2d^\top \bar{y} + \nu \geq \nu_R$ **then**
- 5: $\underline{v} \leftarrow \bar{y}^\top Q \bar{y} + 2d^\top \bar{y} + \nu$ and break; \triangleright Terminate with $\underline{v} \geq \nu_R$.
- 6: **end if**
- 7: $\underline{v} \leftarrow \max(\underline{v}, \bar{y}^\top Q \bar{y} + 2d^\top \bar{y} + \nu)$; \triangleright Keep the best lower bound value ever reached.
- 8: $t \leftarrow \text{DNN_Bound}(Q, d, \nu, F, w)$; \triangleright Compute the DNN bound by solving (15).
- 9: $\bar{v} \leftarrow \min(\bar{v}, t)$; \triangleright Keep the best upper bound value ever obtained.
- 10: **if** $\bar{v} < \nu_R$ **then**
- 11: $\bar{v} \leftarrow \max(\bar{v}, \nu_R - \delta)$ and break; \triangleright Terminate with $\bar{v} < \nu_R$.
- 12: **end if**
- 13: $(Q, d, \nu, F, w) \leftarrow \text{Change_of_Coordinate}(\bar{y}, Q, d, \nu, F, w)$; \triangleright See Algorithm 4.
- 14: $\delta \leftarrow \min(\delta, (\nu_R - \nu)/2)$;
- 15: **for** $i = 1, \dots, k$ **do**
- 16: $\tau_i \leftarrow \frac{Q_{ii}}{-d_i + \sqrt{d_i^2 + Q_{ii}(\nu_R - \delta - \nu)}}$ \triangleright Tuy's cut.
- 17: **end for**
- 18: **for** $i = 1, \dots, k$ **do**
- 19: **if** $\tau_i > 0$ **then**
- 20: $y^i \leftarrow \text{argmax}\{(\tau_i^{-1} Q_i + d)^\top y : F^\top y \leq w, \tau^\top y \geq 1, y \geq 0\}$;
- 21: $\underline{v} \leftarrow \max(\underline{v}, (y^i)^\top Q y^i + 2d^\top y^i + \nu)$;
- 22: **if** $\underline{v} \geq \nu_R$ **then**
- 23: break; \triangleright Terminate with $\underline{v} \geq \nu_R$.
- 24: **end if**
- 25: **end if**
- 26: **end for**
- 27: $\delta \leftarrow \min(\delta, (\nu_R - \underline{v})/2)$;
- 28: $\theta_K \leftarrow \text{Konno_Cut}(Q, d, \nu, F, w, \nu_R, \tau, \delta)$; \triangleright See Algorithm 5.
- 29: **Option I:** $\theta \leftarrow \theta_K$; \triangleright Use Konno's cut.
- 30: **Option II:** $\theta \leftarrow \text{DNN_Cut}(Q, d, \nu, F, w, \nu_R, \tau, \theta_K, \eta, \delta)$; \triangleright See Algorithm 6.
- 31: $F \leftarrow (F - \theta)$, $w \leftarrow \begin{pmatrix} w \\ -1 \end{pmatrix}$; \triangleright Add a valid cut.
- 32: **end while**

Output: upper bound \bar{v} , lower bound \underline{v} such that $\nu_R \notin (\underline{v}, \bar{v}]$.

dynamic reference value $\nu_R = \underline{v} + \epsilon^2$. As a result, there is no harm to cut off any solution with an objective value equal to ν_R , since we must have recorded some points with the same objective value \underline{v} beforehand. Tuy's cut is modified accordingly (line 12). Comparing with line 16 of Algorithm 1, we see that the term $\nu_R - \delta - \nu$ is replaced with $\underline{v} + \epsilon^2 - \nu$. This is because $\nu_R = \underline{v} + \epsilon^2$ and $\delta = 0$ in Algorithm 2. In this case, we cut the region with an objective value bounded by $\underline{v} + \epsilon^2$, which is consistent with our termination criteria (57).

Finally, the lower bound \underline{v} returned by Algorithm 2 corresponds to the objective value of a certain feasible solution of (1). The corresponding solution can be added to the output if needed.

Algorithm 2 QuadProgCD-G

Input: $Q \succeq 0$, $d \in \mathbb{R}^k$, $\nu \in \mathbb{R}$, $F \in \mathbb{R}^{k \times m}$, $w \in \mathbb{R}^m$, relative gap tolerance $\epsilon > 0$, factor $\eta \in (0, 1)$.

- 1: $\underline{v} \leftarrow -\infty$; $\bar{v} \leftarrow \infty$;
- 2: **while** $\bar{v} - \underline{v} > \epsilon \max(|\underline{v}|, \epsilon)$ **do**
- 3: $\bar{y} \leftarrow \text{Search_of_KKT_Point}(Q, d, \nu, F, w)$; ▷ See Algorithm 3.
- 4: $\underline{v} \leftarrow \max(\underline{v}, \bar{y}^\top Q \bar{y} + 2d^\top \bar{y} + \nu)$; ▷ Keep the best lower bound value ever reached.
- 5: $t \leftarrow \text{DNN_Bound}(Q, d, \nu, F, w)$; ▷ Compute the DNN bound by solving (15).
- 6: $\bar{v} \leftarrow \min(\bar{v}, t)$; ▷ Keep the best upper bound value ever reached.
- 7: **if** $\bar{v} \leq \underline{v} + \epsilon \max(|\underline{v}|, \epsilon)$ **then**
- 8: $\bar{v} \leftarrow \max(\bar{v}, \underline{v} + \epsilon^2)$ and break; ▷ Terminate.
- 9: **end if**
- 10: $(Q, d, \nu, F, w) \leftarrow \text{Change_of_Coordinate}(\bar{y}, Q, d, \nu, F, w)$; ▷ See Algorithm 4.
- 11: **for** $i = 1, \dots, k$ **do**
- 12: $\tau_i \leftarrow \frac{Q_{ii}}{-d_i + \sqrt{d_i^2 + Q_{ii}(\underline{v} + \epsilon^2 - \nu)}}$; ▷ Tuy's cut.
- 13: **end for**
- 14: **for** $i = 1, \dots, k$ **do**
- 15: **if** $\tau_i > 0$ **then**
- 16: $y^i \leftarrow \text{argmax}\{(\tau_i^{-1} Q_i + d)^\top y : F^\top y \leq w, \tau^\top y \geq 1, y \geq 0\}$;
- 17: $\underline{v} \leftarrow \max(\underline{v}, (y^i)^\top Q y^i + 2d^\top y^i + \nu)$;
- 18: **if** $\bar{v} - \underline{v} \leq \epsilon \max(|\underline{v}|, \epsilon)$ **then**
- 19: $\bar{v} \leftarrow \max(\bar{v}, \underline{v} + \epsilon^2)$ and break; ▷ Terminate.
- 20: **end if**
- 21: **end if**
- 22: **end for**
- 23: $\theta_K \leftarrow \text{Konno_Cut}(Q, d, \nu, F, w, \underline{v} + \epsilon^2, \tau, 0)$; ▷ See Algorithm 5.
- 24: **Option I:** $\theta \leftarrow \theta_K$; ▷ Use Konno's cut.
- 25: **Option II:** $\theta \leftarrow \text{DNN_Cut}(Q, d, \nu, F, w, \underline{v} + \epsilon^2, \tau, \theta_K, \eta, 0)$; ▷ See Algorithm 6.
- 26: $F \leftarrow (F - \theta)$, $w \leftarrow \begin{pmatrix} w \\ -1 \end{pmatrix}$; ▷ Add a valid cut.
- 27: **end while**

Output: Upper bound \bar{v} , lower bound \underline{v} such that $0 \leq \bar{v} - \underline{v} \leq \epsilon \max(|\underline{v}|, \epsilon)$.

4.3 Computation of the DNN bound

The DNN bound in line 8 of Algorithm 1 and in line 5 of Algorithm 2 can be replaced by any valid upper bound of $\Phi^*(\mathcal{F})$. In fact, as discussed in Section 2.3, it is impossible to compute the exact value of $\Phi(\mathcal{F})$, which corresponds to the optimal value of the SDP problem (15). For high-dimensional problems, even an approximation with high accuracy of $\Phi(\mathcal{F})$ is not accessible due to the memory issue or the time limit. We rely on Proposition 2 for obtaining a valid upper bound of $\Phi^*(\mathcal{F})$ from any approximate SDP solution. Similarly, when we compute the DNN cut in line 30 of Algorithm 1 and in line 25 of Algorithm 2, it suffices to find a valid upper bound of the optimal value of the SDP problem (52) and we again rely on Proposition 2. In this way, Algorithm 1 and Algorithm 2 are open to a wide range of SDP solvers, including in particular those that are able to provide medium accuracy solutions for high dimensional problems. This flexibility is crucial to make QuadProgCD competitive when the problem size increases. The price to pay is the degradation of the quality of the upper bound. Nevertheless, as we will show in the next sec-

tion through extensive numerical tests, the gain appears to outweigh the loss and `QuadProgCD` shows superior performance compared with existing solvers especially for problems with large size.

4.4 Convergence of the algorithm

As the paper is already lengthy, we have decided to leave the study of the convergence properties of Algorithm 1 and Algorithm 2 to future research. Nonetheless, we would like to provide some brief comments on this challenging problem.

Firstly, it is important to note that the lower bound \underline{v} is only guaranteed to be non-decreasing, and the upper bound \bar{v} is only guaranteed to be non-increasing during the iterations. In other words, while adding a valid cut always leads to a strictly smaller feasible region, it may not always result in a strict improvement of the upper or lower bound. Interested readers may refer to the numerical experiments in Figure 5 in the later section, which demonstrate the stagnation of both lower and upper bounds during the iterations.

In fact, finite convergence of a “pure cutting plane method” is hard to be ensured. The best-known result is the finite convergence of Tuy’s cut, which is established under certain conditions; see [13, Theorem V.2]. The condition basically requires that the cuts successively added should be sufficiently large. Without imposing such conditions, even the convergence of Konno’s cut is unknown, according to Chapter V Section 4.2 of [13]. As an alternative, many papers propose the modification of the pure cutting plane method by incorporating cone-splitting, enumerative elements, or branch-and-bound techniques to ensure finite convergence; see [14, 29, 35].

5 Numerical Experiments

In this section, we evaluate the numerical performance of the proposed algorithms `QuadProgCD-R` (Algorithm 1) and `QuadProgCD-G` (Algorithm 2), one for solving the reference value problem (28) and the other for solving globally (1). For the sake of simplicity, when the problem type is clear, we use `QuadProgCD` to refer to both of the two variants. We compare `QuadProgCD` with two commercial solvers `CPLEX` (version 22.1.0)³ and `Gurobi` (version 9.5.0)⁴, and also with an open-source solver `quadprogIP`⁵ which is a nonconvex QP solver proposed very recently in [37].

Our algorithm `QuadProgCD` is implemented and run with `MATLAB R2021a` (version 9.10.0.1851785). In numerical experiments, the interfaces of `CPLEX` and `Gurobi` are called through a Python script. Unless otherwise specified,

³ <https://www.ibm.com/hk-en/analytics/cplex-optimizer>

⁴ <https://www.gurobi.com>

⁵ <https://github.com/xiawei918/quadprogIP>

all the tests are performed on a Windows laptop with Intel(R) Core(TM) i7-8750H CPU 2.20 GHz, 6 cores and 16GB memory. The code of QuadProgCD is available at <https://github.com/tianyouzeng/QuadProgCD>.

5.1 Problem instances

We use both real and synthetic data for experiments. All the instances used for the comparison are uploaded at the above address. We describe them in detail below.

5.1.1 Real data

This set of data has a real application background in computational biology. In [39], the authors proposed an approach to detect new genome or protein sequence based on some known sequence data. A key step in their approach is to solve a set of reference value problems which can be described as

$$\begin{aligned} \max_{x \in \mathbb{R}^n} \quad & x^\top Hx + 2p^\top x \\ \text{s.t.} \quad & Ax = b \\ & x \geq 0, \end{aligned} \tag{58}$$

where $H \in \mathcal{S}^n$ is positive semidefinite, $p \in \mathbb{R}^n$, $A \in \mathbb{R}^{m \times n}$ with $m < n$, and $b \in \mathbb{R}^m$. By elimination of variables, program (58) can be reduced into the form of (1) with $k = n - m$. Due to the very special application background, the matrices and vectors H , p , A , b for describing the concave QP problem (58) are dense. Moreover, all the entries in p , A , b are nonnegative and H is a completely positive matrix.

The data is divided into two groups: one group of dimension $n = 100$ and the other group of dimension $n = 841$. For both groups, the number of rows of A is $m = 22$. Therefore in the reduced form (1), we have $k = 78$ and $k = 819$ for each group respectively. The reference value is fixed to be $n(n+1)(2n+1)/6$ for all the instances. For convenience, we call the two groups BioData100 and BioData841 respectively. For BioData100, there are 317,458 instances, while for BioData841 we have only 3 instances.

5.1.2 Synthetic data

We next consider QP in the format of (58) with randomly generated synthetic data. The matrices and vectors required to define the program are generated as follows. For $k_1, k_2 \in \mathbb{N}$ and $a, b \in \mathbb{R}$, we denote by $\mathcal{U}(k_1, k_2, a, b)$ a random matrix with k_1 rows and k_2 columns such that each entry is a uniform random variable in $[a, b]$ and entries are mutually independent. We first fix the data dimension n , then we generate the feasible region $\mathcal{F} := \{x : Ax = b, x \geq 0\}$ by the following steps:

1. Choose m uniformly randomly from the integers in $[0.1n, 0.5n]$;
2. Generate $A \sim \mathcal{U}(n, m, -20, 20)$;
3. Generate $x_0 \sim \mathcal{U}(n, 1, 0, 1)$;
4. Let $b = Ax_0/\|x_0\|$. If \mathcal{F} is bounded, remove redundant rows of A if necessary and terminate. Otherwise go to step 1.

Such a procedure guarantees that \mathcal{F} is feasible and bounded so that Assumption 1 is satisfied. The objective function Φ is generated as follows:

5. Generate $U \sim \mathcal{U}(n, n, -1, 1)$, $p \sim \mathcal{U}(n, 1, -10, 10)$;
6. Generate $h \sim \mathcal{U}(n, 1, 0, 1)$. Let $D_0 = \text{diag}(h)$ and $H_0 = UD_0U^\top$;
7. Generate $\alpha \sim \mathcal{U}(1, 1, 10, 11)$. Set $H = n\alpha H_0/\|H_0\|$ and $D = n\alpha D_0/\|H_0\|$.

Note that the matrices and vectors generated in this way are dense.

The synthetic data is divided into seven groups: CQMAX20, CQMAX50, CQMAX100, PCQMAX20, PCQMAX50, PCQMAX100 and PCQMAX500. The integer number in the suffix refers to the dimension n of the instance. Instances with prefix CQMAX are generated following the above procedure. Instances with prefix PCQMAX are generated with a small difference in step 2 and 5: $A \sim \mathcal{U}(n, m, 0, 20)$, $U \sim \mathcal{U}(n, n, 0, 1)$ and $p \sim \mathcal{U}(n, 1, 0, 10)$, so that the generated instances have positive entries for each matrix or vector.

For problems of dimension $n \leq 100$, we solve their corresponding reduced concave QP problem (1) by CPLEX or Gurobi to get the value $\Phi^*(\mathcal{F})$ and generate ν_R in a neighborhood of $\Phi^*(\mathcal{F})$. For problem of dimension 500, as we have no access to $\Phi^*(\mathcal{F})$ using CPLEX or Gurobi, we set ν_R to be a random number larger than some known lower bound of $\Phi^*(\mathcal{F})$.

5.2 Numerical results

This subsection is divided into three parts. In the first part (Section 5.2.1 and Section 5.2.2), we present numerical results for solving the reference problem with Algorithm 1. In the second part (Section 5.2.3), we show the numerical results for the global solution of (1) with Algorithm 2. In the third part (Section 5.2.4), we demonstrate the difference between option I (Konno's cut) and option II (DNN cut) in Algorithm 2.

Unless otherwise specified, we let $\eta = 1/2$ and $\delta = 10^{-6}$. The displayed computational time are all measured in seconds. The SDP problems are solved with either MOSEK or SDPNAL+. A valid upper bound based on the solution returned by the SDP solver is then computed using the formula established in Proposition 2.

5.2.1 Reference value problems with real data

In this section, we report the computational results of QuadProgCD-R (Algorithm 1) for solving the reference value problem arising from the new genome or protein detection problem. Recall that we have two groups of instances: BioData100 with 317,458 instances and BioData841 with 3 instances.

For BioData841, the test results are summarized in Table 1. CPLEX and Gurobi both failed to solve these three instances within **1000** seconds, while our algorithm QuadProgCD managed to solve them in less than **40** seconds each. Due to the large dimension $n = 841$, MOSEK fails to terminate in reasonable time limit for the inner SDP problems and we had to adopt SDPNAL+ for solving the inner SDP problems.

Table 1 Comparison of three algorithms on the dataset BioData841. Note that the instance with time equal to 1000 means that the corresponding solver failed to solve it within 1000 seconds.

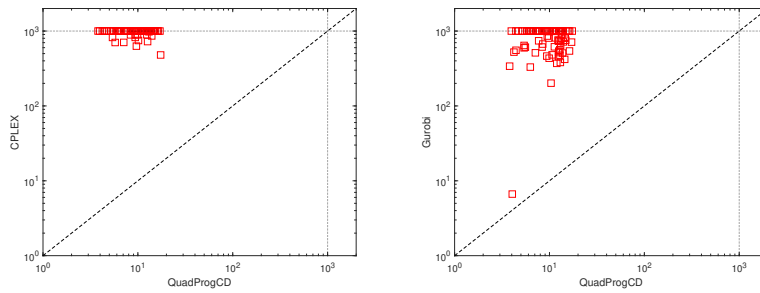
Instance	QuadProgCD Time	CPLEX Time	Gurobi Time
1	36.87	1000	1000
2	0.32	1000	1000
3	36.8	1000	1000

For BioData100, we randomly selected 100 instances out of the 317,458 instances and tested the three algorithms for the reference value problem. The results are displayed in Figure 1. Here we follow the format used in [6] to display the comparison. Each square represents one instance, and its xy -coordinates represent the wall-clock times of the two methods. The diagonal $y = x$ line is plotted in dashed line for reference. If a square is located above the diagonal, QuadProgCD solves the instance faster. The far the square from the diagonal, the larger the ratio between the two wall-clock times. We set the maximum time limit to be 1000 seconds and the dotted horizontal line represents this time limit. If a square sits on the dotted horizontal line in the left (resp. right) plot, it means that CPLEX (resp. Gurobi) is not able to determine whether $\nu_R > \Phi^*(\mathcal{F})$ or $\nu_R \leq \Phi^*(\mathcal{F})$ within 1000 seconds.

From Figure 1, we observe that CPLEX failed to solve most of the instances within **1000** seconds. Gurobi seems to perform better than CPLEX but it also failed to solve about half of the instances within the time limit. In contrast, our algorithm QuadProgCD is able to solve all the 100 instances with an average wall-clock time around **10** seconds.

We also run our algorithm QuadProgCD to solve the reference value problem for all the 317,458 instances of dimension $n = 100$ ($k = 78$) on the HKU High Performance Computing cluster⁶ using 32 processors at the same time. The algorithm successfully solved all the instances within **3 days** (about 5% of them are infeasible instances). However, with CPLEX and Gurobi, the computational time for one single instance may take up to several hours and it is estimated to take **years** of computational time for solving all the 317,458 instances with these two solvers in the same computational environment.

⁶ <https://hpc.hku.hk/hpc/hpc2021/>



(a) QuadProgCD vs CPLEX on BioData100. (b) QuadProgCD vs Gurobi on BioData100.

Fig. 1 Wall-clock time comparison for solving the reference value problem on 100 instances randomly selected from BioData100, plotted in log-log scale.

5.2.2 Reference value problems with synthetic data

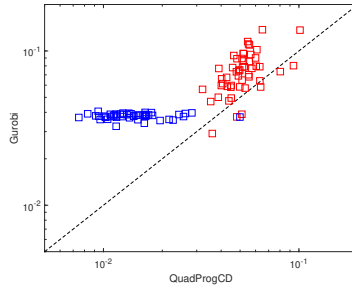
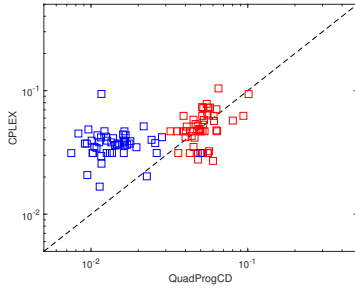
In this section we compare the performance of QuadProgCD-R (Algorithm 1), CPLEX and Gurobi for the reference problem on synthetic data PCQMAX. Each group PCQMAX20, PCQMAX50, PCQMAX100 has 100 instances. The group PCQMAX500 has 10 instances.

For instances of relatively low dimension from the dataset PCQMAX20, PCQMAX50 and PCQMAX100, it is possible to solve the doubly nonnegative relaxation using an interior point method. The results with MOSEK as the SDP solver are summarized in Figure 2. The red squares stand for instances for which $\nu_R > \Phi^*(\mathcal{F})$, while the blue squares stand for instances for which $\nu_R \leq \Phi^*(\mathcal{F})$. It can be observed that QuadProgCD outperforms significantly CPLEX and Gurobi in most of the cases. Moreover, the superior performance of QuadProgCD is more and more remarkable when the dimension increases.

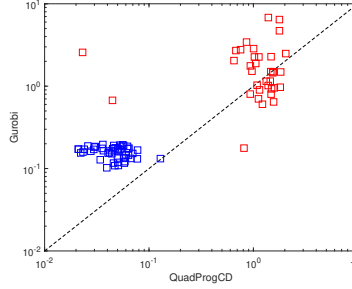
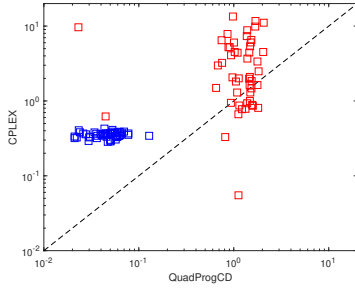
For instances of relatively large dimension from the dataset PCQMAX100 and PCQMAX500, we adopt SDPNAL+ as the SDP solver. The results are displayed in Figure 3. By comparing Figure 2e-2f with Figure 3a-3b, we conclude that QuadProgCD with medium-accuracy SDP solver SDPNAL+ can be faster than QuadProgCD with high-accuracy SDP solver MOSEK on the dataset PCQMAX100. For the dataset PCQMAX500, we set the maximum time limit to be **3600** seconds. It can be seen from Figure 3c and Figure 3d that CPLEX and Gurobi failed on all the 10 instances within the time limit **3600** seconds. In contrast, QuadProgCD solved all the 10 instances of dimension 500 all within **1000** seconds.

5.2.3 Global solution

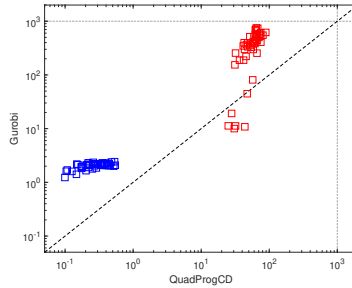
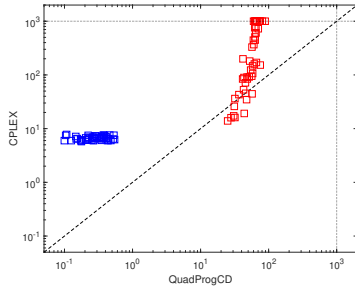
In this section, we compare QuadProgCD-G (Algorithm 2) with three other global solvers CPLEX, Gurobi and quadprogIP for globally solving (1). The relative gap tolerance ϵ in the termination criteria (57) is set to be $\epsilon = 10^{-6}$. The test is performed on samples from the real dataset BioData100 and from



(a) QuadProgCD vs CPLEX on PCQMAX20. (b) QuadProgCD vs Gurobi on PCQMAX20.



(c) QuadProgCD vs CPLEX on PCQMAX50. (d) QuadProgCD vs Gurobi on PCQMAX50.



(e) QuadProgCD vs CPLEX on PCQMAX100. (f) QuadProgCD vs Gurobi on PCQMAX100.

Fig. 2 Wall-clock time comparison for solving the reference value problem on PCQMAX, plotted in log-log scale, where the SDP problem in QuadProgCD is solved by MOSEK.

the synthetic dataset PCQMAX20, PCQMAX50, PCQMAX100, CQMAX20, CQMAX50 and CQMAX100.

Let us examine the performance of the four algorithms on real dataset displayed in Table 2. We randomly selected 20 instances from the 317,458 instances of the dataset BioData100. QuadProgCD reached the gap tolerance $\epsilon = 10^{-6}$ in **hundreds** of seconds for 19 instances. CPLEX reached the gap tolerance $\epsilon = 10^{-6}$ for only 4 instances within the time limit which is set to be

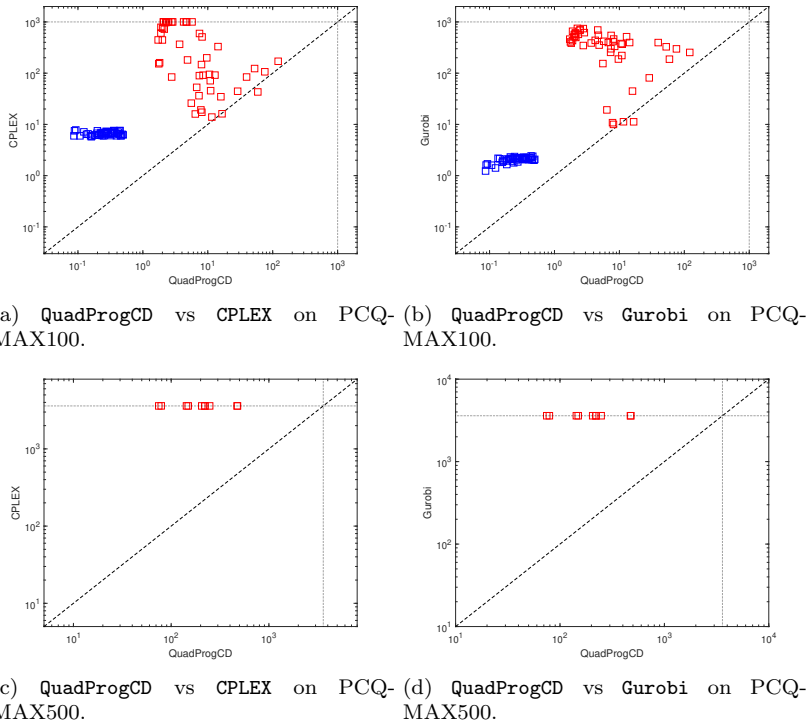


Fig. 3 Wall-clock time comparison for solving the reference value problem on PCQMAX, plotted in log-log scale, where the SDP problem in QuadProgCD is solved inexactly by SDPNAL+.

3600 seconds. Gurobi reached the gap tolerance $\epsilon = 10^{-6}$ for only 6 instances within the time limit. quadprogIP reached the gap tolerance $\epsilon = 10^{-6}$ for only 6 instances within the time limit.

If we examine the performance of the four algorithms on the synthetic dataset in Table 3, we observe that QuadProgCD has comparable short running time with CPLEX for low dimensional instances with $n = 20$. However, when the dimension increases to $n = 100$, QuadProgCD outperforms the other three algorithms by a significant margin in most of the cases.

Finally we demonstrate the long time behavior of the packages QuadProgCD, CPLEX and Gurobi on six selected instances from the real dataset BioData100. The plot of time versus relative gap is shown in Figure 4. It is easy to conclude that QuadProgCD outperforms notably CPLEX and Gurobi both in terms of the convergence speed and in terms of the accuracy that can ever be reached.

More detailed information about QuadProgCD, including the number of iteration and the percentage of wall-clock running time spent on different sub-tasks, is summarized in Appendix F.

Table 2 Comparison of four algorithms on 20 instances from the real dataset BioData100 for reaching the relative gap tolerance $\epsilon = 10^{-6}$. The shortest wall-clock time in each row is in bold font. A hyphen (-) indicates that a gap less than 10^{-6} is reached, and N/A represents that the algorithm fails to obtain an upper or lower bound before the time limit. If a gap less than 10^{-6} is not reached before the time limit, then the achieved gap is displayed in the column RelGap.

Instance	QuadProgCD		CPLEX		Gurobi		quadprogIP	
	RelGap	Time	RelGap	Time	RelGap	Time	RelGap	Time
257424	-	258.88	-	2269.93	-	2233.72	N/A	3600
84896	-	130.18	-	705.71	-	3045.90	N/A	3600
141783	-	203.66	6.94×10^{-2}	3600	1.93×10^{-4}	3600	N/A	3600
123044	-	124.27	1×10^{-1}	3600	2.31×10^{-1}	3600	N/A	3600
303256	-	47.86	2.46×10^{-2}	3600	1.86×10^{-3}	3600	-	151.68
312988	5.85×10^{-5}	3600	-	1486.21	9.54×10^{-5}	3600	N/A	3600
229644	-	57.92	8.78×10^{-2}	3600	2.55×10^{-1}	3600	N/A	3600
259490	-	47.21	1.25×10^{-1}	3600	8.64×10^{-4}	3600	N/A	3600
143339	-	124.83	8.62×10^{-2}	3600	-	1759.16	N/A	3600
95618	-	334.64	2.58×10^{-2}	3600	1.71×10^{-4}	3600	N/A	3600
23659	-	47.33	1.45×10^{-1}	3600	2.97×10^{-1}	3600	-	901.61
284341	-	434.11	9.83×10^{-2}	3600	6.51×10^{-3}	3600	N/A	3600
79834	-	113.41	1.39×10^{-1}	3600	1.06×10^{-3}	3600	-	36.23
88552	-	55.56	3.13×10^{-2}	3600	1.69×10^{-1}	3600	-	143.80
305293	-	772.30	2.82×10^{-3}	3600	8.69×10^{-4}	3600	-	124.47
149864	-	54.02	3.55×10^{-2}	3600	6.69×10^{-2}	3600	N/A	3600
81426	-	673	5.47×10^{-2}	3600	7.20×10^{-5}	3600	N/A	3600
274863	-	125.34	-	1093.11	-	3220.62	N/A	3600
82857	-	124.21	3.83×10^{-2}	3600	-	2335.98	-	1056.03
211213	-	204.01	2.65×10^{-2}	3600	-	2076.43	N/A	3600

5.2.4 Comparison between Konno's cut and DNN cut

Recall that Theorem 2 states:

$$\bar{\phi}_{\tau,\theta}^K \geq \bar{\phi}_{\tau,\theta}^L \geq \bar{\phi}_{\tau,\theta}^D \geq \phi_{\tau,\theta}^*, \quad \forall \theta \geq 0. \quad (59)$$

We calculate the relative improvement of the LP relaxation bound and the DNN relaxation bound, which are defined by

$$\text{RI}_L(\theta_K) := \frac{\bar{\phi}_{\tau,\theta_K}^K - \bar{\phi}_{\tau,\theta_K}^L}{\bar{\phi}_{\tau,\theta_K}^K}, \quad \text{RI}(\theta_K) := \frac{\bar{\phi}_{\tau,\theta_K}^K - \bar{\phi}_{\tau,\theta_K}^D}{\bar{\phi}_{\tau,\theta_K}^K}.$$

Note that (59) implies that

$$0 \leq \text{RI}_L(\theta_K) \leq \text{RI}(\theta_K) \leq 1. \quad (60)$$

Let us verify (60) with numerical experiments. We randomly selected 20 instances from the real dataset BioData100 and run one iteration of QuadProgCD. We display the values of $(\text{RI}_L(\theta_K), \text{RI}(\theta_K))$ in Table 4 for those instances with nonempty feasible region after adding Konno's cut.

To demonstrate the impact on generation of deeper cuts, we show in Table 5 the acceptance/rejection rate of the deepened cut $\theta = \theta_K/2$ under the criteria $\bar{\phi}_{\tau,\theta}^L \leq \nu_R - \delta$ and $\bar{\phi}_{\tau,\theta}^D \leq \nu_R - \delta$ over the dataset PCQMAX and CQMAX.

Table 3 Comparison of four algorithms on synthetic data PCQMAX and CQMAX for reaching the relative gap tolerance $\epsilon = 10^{-6}$. The shortest wall-clock time in each row is in bold font. A hyphen (-) indicates that a gap less than 10^{-6} is reached, and N/A represents that the algorithm fails to obtain an upper or lower bound before the time limit. If a gap less than 10^{-6} is not reached before the time limit, then the achieved gap is displayed in the column RelGap.

Instance	QuadProgCD		CPLEX		Gurobi		quadprogIP	
	RelGap	Time	RelGap	Time	RelGap	Time	RelGap	Time
pcqmax20-1	-	0.08	-	0.08	-	0.20	-	0.98
pcqmax20-2	-	0.10	-	0.05	-	0.07	-	0.13
pcqmax20-3	-	0.17	-	0.07	-	0.10	-	0.98
pcqmax20-4	-	0.15	-	0.06	-	0.11	-	1.07
pcqmax20-5	-	0.03	-	0.03	-	0.06	-	0.13
pcqmax20-6	-	0.07	-	0.03	-	0.09	-	0.42
pcqmax20-7	-	0.31	-	0.05	-	0.07	-	0.13
pcqmax20-8	-	0.09	-	0.08	-	0.12	-	0.44
pcqmax20-9	-	0.10	-	0.05	-	0.08	-	1.19
pcqmax20-10	-	0.08	-	0.06	-	0.08	-	1.08
pcqmax50-1	-	1.38	-	4.27	-	41.47	N/A	3600
pcqmax50-2	-	1.06	-	13.11	-	34.78	N/A	3600
pcqmax50-3	-	2.62	-	9.63	-	42.38	N/A	3600
pcqmax50-4	-	2.53	-	11.77	-	35.97	N/A	3600
pcqmax50-5	-	2.45	-	4.79	-	40.08	N/A	3600
pcqmax50-6	-	2.57	-	6.05	-	60.76	N/A	3600
pcqmax50-7	-	0.50	-	0.55	-	0.80	-	31.83
pcqmax50-8	-	0.94	-	4.40	-	52.33	N/A	3600
pcqmax50-9	-	0.63	-	1.15	-	1.85	-	73.36
pcqmax50-10	-	2.26	-	1.53	-	7.84	N/A	3600
pcqmax100-1	-	53.79	-	76.38	-	337.77	N/A	3600
pcqmax100-2	-	96.99	-	3380.71	-	3427.90	N/A	3600
pcqmax100-3	-	122.83	-	94.42	-	550.03	N/A	3600
pcqmax100-4	-	48.37	-	45.88	-	298.55	N/A	3600
pcqmax100-5	-	65.96	-	100.63	-	358.33	N/A	3600
pcqmax100-6	-	178.47	1.87×10^{-2}	3600	-	2576.43	N/A	3600
pcqmax100-7	-	148.27	-	856.33	-	802.37	N/A	3600
pcqmax100-8	-	77.36	-	86.75	-	479.76	N/A	3600
pcqmax100-9	-	106.64	-	2738.93	-	2261.27	N/A	3600
pcqmax100-10	-	92.37	-	48.94	-	367.20	N/A	3600
Instance	RelGap	Time	RelGap	Time	RelGap	Time	RelGap	Time
cqmax20-1	-	0.09	-	0.07	-	134.77	-	1.52
cqmax20-2	-	0.08	-	0.03	-	445.84	-	0.38
cqmax20-3	-	0.08	-	0.07	-	73.46	-	0.94
cqmax20-4	-	0.11	-	0.04	-	10.38	-	0.53
cqmax20-5	-	0.07	-	0.03	-	231.45	-	1.33
cqmax20-6	-	0.08	-	0.06	-	11.38	-	0.68
cqmax20-7	-	0.16	-	0.08	-	90.88	-	1.20
cqmax20-8	-	0.07	-	0.04	-	1932.81	-	0.57
cqmax20-9	-	0.08	-	0.05	-	10.62	-	1.38
cqmax20-10	-	0.07	-	0.06	-	26.91	-	1.45
cqmax50-1	-	1.14	-	1.28	N/A	3600	N/A	3600
cqmax50-2	-	2.40	-	1.29	N/A	3600	N/A	3600
cqmax50-3	-	2.60	-	1.86	N/A	3600	N/A	3600
cqmax50-4	-	1.27	-	1.61	N/A	3600	N/A	3600
cqmax50-5	-	3.02	-	3.44	N/A	3600	N/A	3600
cqmax50-6	-	2.80	-	5.58	N/A	3600	N/A	3600
cqmax50-7	-	2.38	-	3.16	N/A	3600	N/A	3600
cqmax50-8	-	3.29	-	5.99	N/A	3600	N/A	3600
cqmax50-9	-	1	-	1.97	N/A	3600	N/A	3600
cqmax50-10	-	0.84	-	2.24	N/A	3600	N/A	3600
cqmax100-1	-	109.85	-	322.51	N/A	3600	N/A	3600
cqmax100-2	-	39.83	-	108.96	N/A	3600	N/A	3600
cqmax100-3	-	107.91	-	253.22	N/A	3600	N/A	3600
cqmax100-4	-	116.20	-	514.25	N/A	3600	N/A	3600
cqmax100-5	-	30.90	-	328.38	N/A	3600	N/A	3600
cqmax100-6	-	187.58	-	922.90	N/A	3600	N/A	3600
cqmax100-7	-	101.41	-	540.52	N/A	3600	N/A	3600
cqmax100-8	-	309.48	7.18×10^{-5}	3600	N/A	3600	N/A	3600
cqmax100-9	-	196.82	2.38×10^{-3}	3600	N/A	3600	N/A	3600
cqmax100-10	-	115.48	-	696.97	N/A	3600	N/A	3600

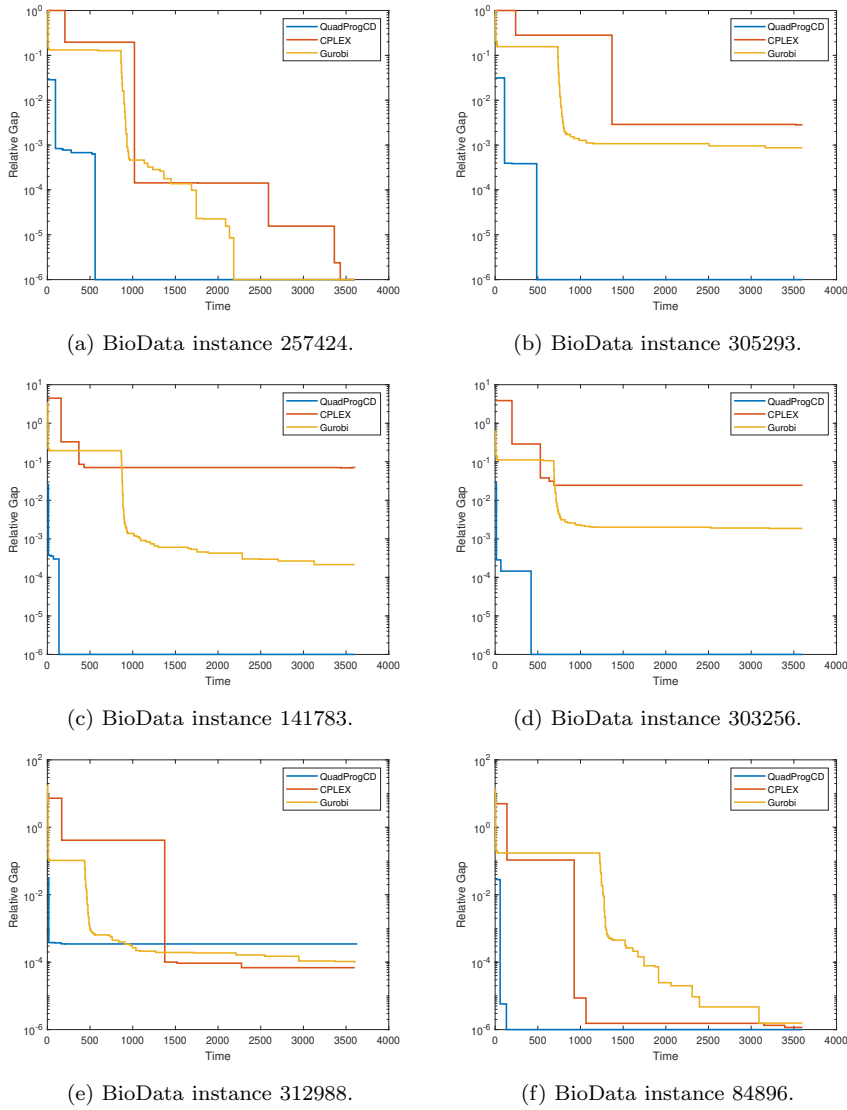


Fig. 4 Convergence behaviour of three algorithms, with relative gap $(\bar{v} - \underline{v})/|\underline{v}|$ plotted in log scale.

The second column displays the number of instances with nonempty feasible region after adding Konno's cut in the first iteration of **QuadProgCD**. The third column displays the percentage of the instances which satisfy $\bar{\phi}_{\tau, \theta}^L \leq \nu_R - \delta$ and the fourth column displays the percentage of the instances which satisfy $\bar{\phi}_{\tau, \theta}^D \leq \nu_R - \delta$.

Table 4 Comparison of different relaxation bounds.

Instance Index	$RI_L(\theta_K)$	$RI(\theta_K)$
465	0.0207	0.0208
1582	0.0143	0.0152
4455	0.0163	0.0164
4571	0.0163	0.0169
6664	0.0096	0.0156
8946	0.0172	0.0172
9217	0.0112	0.0142
10824	0.0182	0.0198
11114	0.0127	0.0142
11669	0.0142	0.0153

Table 5 Acceptance/rejection rates of the deepened cut $\theta := \theta_K/2$ using different criteria. Here, a valid instance refers to an instance which is feasible after adding a Konno's cut.

Dataset	Valid instances	Valid LR Cut	Valid DNNR Cut
PCQMAX20	11	100.00%	100.00%
PCQMAX50	62	98.39%	100.00%
PCQMAX100	97	89.69%	85.57%
CQMAX20	19	89.47%	100.00%
CQMAX50	57	82.46%	91.23%
CQMAX100	75	64.00%	82.67%

Remark 6 In Table 5, it can be observed that the percentage of valid LR cuts is higher than that of valid DNNR cuts for the dataset PCQMAX100, which appears to contradict the inequality $\bar{\phi}_{\tau,\theta}^D \leq \bar{\phi}_{\tau,\theta}^L$ established in Theorem 2. This is due to the fact that numerical solvers cannot return the exact values of $\bar{\phi}_{\tau,\theta}^D$. To this end, we used the upper bound in (22) instead of the exact value of $\bar{\phi}_{\tau,\theta}^D$ in our computation. This upper bound of $\bar{\phi}_{\tau,\theta}^D$ may occasionally exceed the value of $\bar{\phi}_{\tau,\theta}^L$, resulting in LR cuts exhibiting better performance than DNNR cuts.

Finally, we compare the performance of Option I (Konno's cut) with Option II (DNN cut). We randomly selected 20 instances from the real dataset Biodata100 and set $\eta = 1/10$ in this experiment. The termination criterion is the reach of a relative gap $\epsilon = 10^{-6}$. The time limit is set to be 1000 seconds. The result is summarized in Table 6. It can be seen that Option II is superior than Option I in most of the cases, which confirms the effectiveness of the proposed strategy of deepening Konno's cut through the LP and DNN relaxation.

6 Conclusion

In this paper, we develop an efficient global solver for the concave QP problem (1), which is known to be an NP-hard problem. The concave QP problem

Table 6 Comparison of Option I and with Option II in QuadProgCD-R. The time limit is set to 1000 seconds. The shortest wall-clock time in each row is in bold font.

Instance	Option I	Option II
252565	32.99	18.54
280796	103.45	38.21
283147	474.75	40.65
196032	288.48	189.81
30238	35.75	21.87
86335	37.40	17.80
169534	107.67	21.17
299116	53.08	18.46
48861	1000.00	1000.00
150467	40.62	25.72
248087	87.00	26.14
43985	105.71	24.30
130746	1000.00	296.92
283879	1000.00	347.46
245585	465.54	25.97
203280	241.20	67.04
11071	58.82	21.99
263231	1000.00	1000.00
289538	39.22	24.45
210408	34.07	54.26

finds a recent application in computational biology, where the associated reference value problem needs to be solved for a huge number (317,584) of instances of dimension 78. The existing QP solvers such as CPLEX or Gurobi seem to require years of computational time for this particular task. By revisiting the classical cutting plane method proposed by Tuy and Konno, we propose to construct deeper cuts through the DNN relaxation. We prove that the DNN relaxation is equivalent to the Shor relaxation of an equivalent QCQP problem. This allows us to write down an SDP formulation of the DNN relaxation which satisfies Slater’s condition, which is crucial for the robustness of applying the existing SDP solvers to compute the DNN bound. We also provide the explicit formula for obtaining a valid upper bound from any approximate primal and dual solution. The proposed algorithm is tested on a variety of real and synthetic instances and outperforms CPLEX, Gurobi and quadprogIP in most of the cases. In particular, our method successfully solved all the 317,584 instances within 3 days on the HKU HPC cluster using 32 processors. Moreover, our algorithm demonstrates superior performance on large-scale instances of dimension up to 819.

Acknowledgements We are deeply grateful to the anonymous referees for their careful reading and their many constructive comments, which helped us improve this paper. The authors would like to thank Prof. Stephen S.-T. Yau for introducing the application of concave QP in computational biology and providing the dataset. We also thank Ms. Xinyuan Zhang for the proofreading work. Parts of computations were performed using research computing facilities offered by Information Technology Services, the University of Hong Kong.

Funding The work of the authors was supported by NSFC Young Scientist Fund grant 12001458 and Hong Kong Research Grants Council grant 17317122.

Author contributions All authors contributed to the study conception and design. Implementation, data generation and numerical experiments were performed by Tianyou Zeng and Yuchen Lou. The first draft of the manuscript was written by Zheng Qu and all authors commented on previous versions of the manuscript. All authors read and approved the final manuscript.

Data Availability Statement The datasets generated during and/or analysed during the current study are available in the repository <https://github.com/tianyouzeng/QuadProgCD>.

Code Availability The full code was reviewed and is available on GitHub at the following address: <https://github.com/tianyouzeng/QuadProgCD>.

Conflict of interest The authors have no relevant financial or non-financial interests to disclose.

References

1. Baesens, B., Van Gestel, T., Viaene, S., Stepanova, M., Suykens, J., Vanthienen, J.: Benchmarking state-of-the-art classification algorithms for credit scoring. *Journal of the Operational Research Society* **54**(6), 627–635 (2003)
2. Burer, S.: Copositive programming. In: M.F. Anjos, J.B. Lasserre (eds.) *Handbook on Semidefinite, Conic and Polynomial Optimization*, pp. 201–218. Springer New York, NY (2012)
3. Burer, S., Vandembussche, D.: A finite branch-and-bound algorithm for nonconvex quadratic programming via semidefinite relaxations. *Mathematical Programming* **113**(2), 259–282 (2008)
4. Burkard, R.E., Cela, E., Pardalos, P.M., Pitsoulis, L.S.: The quadratic assignment problem. In: D.Z. Du, P.M. Pardalos (eds.) *Handbook of Combinatorial Optimization*, pp. 1713–1809. Springer (1998)
5. Cabot, A.V., Francis, R.L.: Solving certain nonconvex quadratic minimization problems by ranking the extreme points. *Operations Research* **18**(1), 82–86 (1970)
6. Chen, J., Burer, S.: Globally solving nonconvex quadratic programming problems via completely positive programming. *Mathematical Programming Computation* **4**(1), 33–52 (2012)
7. Fung, G.: The disputed federalist papers: SVM feature selection via concave minimization. In: *Proceedings of the 2003 Conference on Diversity in Computing*, pp. 42–46 (2003)
8. Gondzio, J., Yıldırım, E.A.: Global solutions of nonconvex standard quadratic programs via mixed integer linear programming reformulations. *Journal of Global Optimization* **81**(2), 293–321 (2021)
9. Guisewite, G.M., Pardalos, P.M.: Minimum concave-cost network flow problems: Applications, complexity, and algorithms. *Annals of Operations Research* **25**(1), 75–99 (1990)
10. Hladík, M., Hartman, D.: Maximization of a convex quadratic form on a polytope: Factorization and the chebyshev norm bounds. In: H.A. Le Thi, H.M. Le, T. Pham Dinh (eds.) *Optimization of Complex Systems: Theory, Models, Algorithms and Applications*, pp. 119–127. Springer International Publishing, Cham (2020)
11. Hladík, M., Hartman, D., Zamani, M.: Maximization of a PSD quadratic form and factorization. *Optimization Letters* **15**(7), 2515–2528 (2021)
12. Horst, R., Pardalos, P.M.: *Handbook of Global Optimization*, vol. 2. Springer Science & Business Media (2013)
13. Horst, R., Tuy, H.: *Global Optimization: Deterministic Approaches*. Springer Science & Business Media (2013)
14. Jacobsen, S.E.: Convergence of a Tuy-type algorithm for concave minimization subject to linear inequality constraints. *Applied Mathematics and Optimization* **7**, 1–9 (1981)

15. Jiao, X., Pei, S., Sun, Z., Kang, J., Yau, S.S.T.: Determination of the nucleotide or amino acid composition of genome or protein sequences by using natural vector method and convex hull principle. *Fundamental Research* **1**(5), 559–564 (2021)
16. Kim, S., Kojima, M., Toh, K.C.: A Lagrangian–DNN relaxation: a fast method for computing tight lower bounds for a class of quadratic optimization problems. *Mathematical Programming* **156**(1), 161–187 (2016)
17. Konno, H.: A cutting plane algorithm for solving bilinear programs. *Mathematical Programming* **11**(1), 14–27 (1976)
18. Konno, H.: Maximization of a convex quadratic function under linear constraints. *Mathematical Programming* **11**(1), 117–127 (1976)
19. Liuzzi, G., Locatelli, M., Piccialli, V.: A computational study on QP problems with general linear constraints. *Optimization Letters* **16**(6), 1633–1647 (2022)
20. Luo, Z.Q., Ma, W.K., So, A.M.C., Ye, Y., Zhang, S.: Semidefinite relaxation of quadratic optimization problems. *IEEE Signal Processing Magazine* **27**(3), 20–34 (2010)
21. Mangasarian, O.L., Street, W.N., Wolberg, W.H.: Breast cancer diagnosis and prognosis via linear programming. *Operations Research* **43**(4), 570–577 (1995)
22. McCormick, G.P.: Computability of global solutions to factorable nonconvex programs: Part I—Convex underestimating problems. *Mathematical Programming* **10**(1), 147–175 (1976)
23. Momoh, J., Dias, L., Guo, S., Adapa, R.: Economic operation and planning of multi-area interconnected power systems. *IEEE Transactions on Power Systems* **10**(2), 1044–1053 (1995)
24. Nesterov, Y.: Semidefinite relaxation and nonconvex quadratic optimization. *Optimization Methods and Software* **9**(1-3), 141–160 (1998)
25. Nohra, C.J., Raghunathan, A.U., Sahinidis, N.: Spectral relaxations and branching strategies for global optimization of mixed-integer quadratic programs. *SIAM Journal on Optimization* **31**(1), 142–171 (2021)
26. Pardalos, P.M., Rosen, J.B.: Methods for global concave minimization: a bibliographic survey. *SIAM Review* **28**(3), 367–379 (1986)
27. Pardalos, P.M., Vavasis, S.A.: Quadratic programming with one negative eigenvalue is NP-hard. *Journal of Global Optimization* **1**(1), 15–22 (1991)
28. Pataki, G.: Characterizing bad semidefinite programs: Normal forms and short proofs. *SIAM Review* **61**(4), 839–859 (2019)
29. Porembski, M.: Finitely convergent cutting planes for concave minimization. *Journal of Global Optimization* **20**(2), 109–132 (2001)
30. Sun, D., Toh, K.C., Yuan, Y., Zhao, X.Y.: SDPNAL+: A Matlab software for semidefinite programming with bound constraints (version 1.0). *Optimization Methods and Software* **35**(1), 87–115 (2020)
31. Telli, M., Bentobache, M., Mokhtari, A.: A successive linear approximation algorithm for the global minimization of a concave quadratic program. *Computational and Applied Mathematics* **39**(4), 1–28 (2020)
32. Toh, K.C., Todd, M.J., Tütüncü, R.H.: SDPT3 — A Matlab software package for semidefinite programming, version 1.3. *Optimization Methods and Software* **11**(1-4), 545–581 (1999)
33. Tuy, H.: Concave programming under linear constraints. *Soviet Math.* **5**, 1437–1440 (1964)
34. Tuy, H.: Nonconvex quadratic programming. In: *Convex Analysis and Global Optimization*, pp. 337–390. Springer (2016)
35. Van Thoai, N., Tuy, H.: Convergent algorithms for minimizing a concave function. *Mathematics of Operations Research* **5**(4), 556–566 (1980)
36. Wen, Z., Goldfarb, D., Yin, W.: Alternating direction augmented Lagrangian methods for semidefinite programming. *Mathematical Programming Computation* **2**(3), 203–230 (2010)
37. Xia, W., Vera, J.C., Zuluaga, L.F.: Globally solving nonconvex quadratic programs via linear integer programming techniques. *INFORMS Journal on Computing* **32**(1), 40–56 (2020)
38. Zamani, M.: A new algorithm for concave quadratic programming. *Journal of Global Optimization* **75**(3), 655–681 (2019)

39. Zhao, R., Pei, S., Yau, S.S.T.: New genome sequence detection via natural vector convex hull method. *IEEE/ACM Transactions on Computational Biology and Bioinformatics* (2020)

A Search of KKT Vertex

Consider problem (1). We first define the bilinear function $\Psi : \mathbb{R}^k \times \mathbb{R}^k \rightarrow \mathbb{R}$ as follows:

$$\Psi(y, \tilde{y}) := y^\top Q \tilde{y} + d^\top y + d^\top \tilde{y} + \nu, \quad \forall y, \tilde{y} \in \mathbb{R}^k. \quad (61)$$

By simple algebra,

$$\Psi(y, \tilde{y}) = \Phi(y) + \frac{1}{2} \langle \nabla \Phi(y), \tilde{y} - y \rangle = \Phi(\tilde{y}) + \frac{1}{2} \langle \nabla \Phi(\tilde{y}), y - \tilde{y} \rangle, \quad \forall y, \tilde{y} \in \mathbb{R}^k. \quad (62)$$

It then follows that

$$\Psi(y, \tilde{y}) = \frac{\Phi(y) + \Phi(\tilde{y})}{2} - \frac{1}{4} \langle \nabla \Phi(y) - \nabla \Phi(\tilde{y}), y - \tilde{y} \rangle \leq \frac{\Phi(y) + \Phi(\tilde{y})}{2}, \quad \forall y, \tilde{y} \in \mathbb{R}^k, \quad (63)$$

where the inequality follows from the convexity of Φ . Based on (63), we immediately have the following result; see [18, Thm 2.2].

Theorem 3 ([18]) *For any subset $\mathcal{Y} \subset \mathbb{R}^k$, we have*

$$\max_{y \in \mathcal{Y}} \Phi(y) = \max_{y \in \mathcal{Y}, \tilde{y} \in \mathcal{Y}} \Psi(y, \tilde{y}).$$

Theorem 3 implies that (1) is equivalent to the following bilinear program.

$$\begin{aligned} \max \quad & \Psi(y, \tilde{y}) \\ \text{s.t.} \quad & y \in \mathcal{F}, \quad \tilde{y} \in \mathcal{F}. \end{aligned} \quad (64)$$

In [17], Konno proposed a *mountain climbing* algorithm for (64), which corresponds to alternatively maximizing over y and \tilde{y} . We define $V(\mathcal{F})$ as the set of vertices of \mathcal{F} .

Algorithm 3 Mountain Climbing Algorithm [17] (Search_of_KKT_Point)

Input: Initial point $y^0 \in \mathbb{R}^k$, feasible region $\mathcal{F} := \{y \in \mathbb{R}^k : Fy \leq w, y \geq 0\}$, bilinear function $\Psi(y, \tilde{y}) := y^\top Q \tilde{y} + d^\top y + d^\top \tilde{y} + \nu$.

```

1:  $\bar{y} \leftarrow y^0$ 
2: while true do
3:    $\tilde{y} \in V(\mathcal{F}) \cap \operatorname{argmax}\{\Psi(y, \bar{y}) : y \in \mathcal{F}\}$ 
4:   if  $\Psi(\tilde{y}, \tilde{y}) = \Psi(\bar{y}, \bar{y})$  then
5:     break;
6:   end if
7:    $\bar{y} \leftarrow \tilde{y}$ 
8: end while

```

Output: $\bar{y} \in V(\mathcal{F})$ such that

$$\bar{y} \in V(\mathcal{F}) \cap \operatorname{argmax}\{\Psi(\bar{y}, y) : y \in \mathcal{F}\}. \quad (65)$$

Since $V(\mathcal{F})$ is a finite set, Algorithm 3 terminates in finitely many iterations. The main computational step of Algorithm 3 is line 3, where one needs to solve an LP problem. Also note that the starting point y^0 is not required to be a feasible solution. In view of (62), (65) is equivalent to (8). Therefore, the output \bar{y} of Algorithm 3 is a KKT vertex of problem (1).

B Change of Coordinate

In this section, we discuss the reformulation of the original QP (1) so that it satisfies the assumptions (29). Let \bar{y} be any KKT vertex of the original problem (1). Without loss of generality we assume $\Phi(\bar{y}) < \nu_R$, otherwise the reference value problem is solved.

We lift the original problem (1) into \mathbb{R}^n as in (4), which can be written as

$$\begin{aligned} \max_{x \in \mathbb{R}^n} \quad & x^\top Hx + 2p^\top x + \nu \\ \text{s.t.} \quad & Ax = b \\ & x \geq 0. \end{aligned} \quad (66)$$

where $H := \begin{pmatrix} Q & \mathbf{0} \\ \mathbf{0}^\top & 0 \end{pmatrix}$, $p := \begin{pmatrix} d \\ \mathbf{0} \end{pmatrix}$, $A := (F^\top \mathbf{I})$ and $b = w$. Since \bar{y} is a KKT vertex of (1), $\bar{x} := \begin{pmatrix} \bar{y} \\ w - F^\top \bar{y} \end{pmatrix}$ is a KKT point of (66) and also a vertex of the feasible region of (66). Let $c = H\bar{x} + p$. Then \bar{x} is a basic feasible solution as well as an optimal solution of the following LP problem:

$$\begin{aligned} \max_{x \in \mathbb{R}^n} \quad & c^\top x \\ \text{s.t.} \quad & Ax = b \\ & x \geq 0. \end{aligned} \quad (67)$$

Let $\{i_1, \dots, i_m\}$ be the indices of basic variables of \bar{x} and $\{j_1, \dots, j_{n-m}\}$ be the indices of nonbasic variables. Note that the choice of basic variables is not unique if \bar{x} is a degenerate vertex. Let $B := (A_{i_1} \cdots A_{i_m})$ be the basis matrix and $N := (A_{j_1} \cdots A_{j_{n-m}})$ be the nonbasis matrix. Following the standard notations in linear programming, for any vector $x \in \mathbb{R}^n$ we denote by x_B the subvector $(x_{i_1}, \dots, x_{i_m}) \in \mathbb{R}^m$ and by x_N the subvector $(x_{j_1}, \dots, x_{j_{n-m}}) \in \mathbb{R}^{n-m}$. Further, we partition accordingly the matrix H and vector p into blocks:

$$\begin{pmatrix} H_{BB} & H_{BN} \\ H_{BN}^\top & H_{NN} \end{pmatrix}, \quad \begin{pmatrix} p_B \\ p_N \end{pmatrix}. \quad (68)$$

By the feasibility and optimality of \bar{x} as a solution of (67), there exists a basis matrix B associated with \bar{x} such that

$$\bar{x}_B = B^{-1}b \geq 0, \quad \bar{x}_N = 0, \quad (69a)$$

$$c_B^\top B^{-1}N - c_N^\top \geq 0. \quad (69b)$$

Given such choice of basis B , for any feasible solution x of (66), we have

$$\begin{aligned} & x^\top Hx + 2p^\top x + \nu \\ &= (x_B^\top \ x_N^\top) \begin{pmatrix} H_{BB} & H_{BN} \\ H_{BN}^\top & H_{NN} \end{pmatrix} \begin{pmatrix} x_B \\ x_N \end{pmatrix} + 2(p_B^\top \ p_N^\top) \begin{pmatrix} x_B \\ x_N \end{pmatrix} + \nu \\ &= \left((B^{-1}(b - Nx_N))^\top \ x_N^\top \right) \begin{pmatrix} H_{BB} & H_{BN} \\ H_{BN}^\top & H_{NN} \end{pmatrix} \begin{pmatrix} B^{-1}(b - Nx_N) \\ x_N \end{pmatrix} \\ &\quad + 2(p_B^\top \ p_N^\top) \begin{pmatrix} B^{-1}(b - Nx_N) \\ x_N \end{pmatrix} + \nu \\ &= x_N^\top \tilde{Q} x_N + 2\tilde{d}^\top x_N + \tilde{\nu} \end{aligned} \quad (70)$$

where

$$\begin{aligned} \tilde{Q} &= H_{NN} + (B^{-1}N)^\top H_{BB} B^{-1}N - (B^{-1}N)^\top H_{BN} - H_{BN}^\top B^{-1}N, \\ \tilde{d} &= p_N + H_{BN}^\top B^{-1}b - (B^{-1}N)^\top p_B - (B^{-1}N)^\top H_{BB} B^{-1}b, \\ \tilde{\nu} &= (B^{-1}b)^\top H_{BB} (B^{-1}b) + 2p_B^\top (B^{-1}b) + \nu. \end{aligned} \quad (71)$$

Then (66) can be rewritten equivalently as follows:

$$\begin{aligned} \max_{y \in \mathbb{R}^k} \quad & y^\top \tilde{Q}y + 2\tilde{d}^\top y + \tilde{\nu} \\ \text{s.t.} \quad & \tilde{F}^\top y \leq \tilde{w} \\ & y \geq 0 \end{aligned} \quad (72)$$

where

$$\tilde{F} := (B^{-1}N)^\top, \quad \tilde{w} := B^{-1}b \geq 0. \quad (73)$$

Recall that

$$c_B = (H\bar{x} + p)_B = H_{BB}B^{-1}b + p_B, \quad c_N = (H\bar{x} + p)_N = H_{BN}^\top B^{-1}b + p_N.$$

Thus

$$c_B^\top B^{-1}N - c_N^\top = (H_{BB}B^{-1}b + p_B)^\top B^{-1}N - (H_{BN}^\top B^{-1}b + p_N)^\top = (-\tilde{d})^\top,$$

and it follows from (69b) that $\tilde{d} \leq 0$. We also know that

$$\Phi(\bar{y}) = \bar{x}^\top H\bar{x} + 2p^\top \bar{x} + \nu = \tilde{\nu}, \quad (74)$$

where the first equality can be checked from the definition of H and \bar{x} , the second equality follows from (70) and the fact that $\bar{x}_N = 0$. Hence we have $\tilde{\nu} < \nu_R$. Therefore (72) is an equivalent model of (1) and it satisfies $\tilde{w} \geq 0$, $\tilde{d} \leq 0$, $\tilde{\nu} < \nu_R$. The above transformation procedure is summarized in Algorithm 4.

Algorithm 4 Change_of_Coordinate

Input: KKT vertex $\bar{y} \in \mathbb{R}^k$, matrix $Q \in \mathcal{S}^k$, vector $d \in \mathbb{R}^k$, constant $\nu \in \mathbb{R}$, matrix $F \in \mathbb{R}^{k \times m}$, vector $w \in \mathbb{R}^m$.

1: $H \leftarrow \begin{pmatrix} Q & \mathbf{0} \\ \mathbf{0}^\top & 0 \end{pmatrix}$, $p \leftarrow \begin{pmatrix} d \\ \mathbf{0} \end{pmatrix}$, $A \leftarrow (F^\top \mathbf{I})$, $b \leftarrow w$.

2: $\bar{x} \leftarrow \begin{pmatrix} \bar{y} \\ w - F^\top \bar{y} \end{pmatrix}$.

3: $c \leftarrow H\bar{x} + p$.

4: Choose basis matrix B and non-basis matrix N associated with \bar{x} such that (69) holds.

5: Compute $(\tilde{Q}, \tilde{d}, \tilde{F}, \tilde{w}, \tilde{\nu})$ according to (71) and (73).

Output: $(\tilde{Q}, \tilde{d}, \tilde{F}, \tilde{w}, \tilde{\nu})$.

C Proof of Lemma 7

Proof (proof of Lemma 7) Note that $\tau_i = 0$ if and only if $Q_{ii} = 0$. Therefore, we have $Q_{11} = \dots = Q_{\ell\ell} = 0$. Since $Q \succeq 0$, the first ℓ columns of Q are all zero vectors, i.e., $Q_1 = \dots = Q_\ell = \mathbf{0}$. It follows that for any scalar $\eta \geq 0$ we have

$$\begin{aligned} g(\eta^{-1}e_i) &= \max\{(\eta^{-1}Q_i + d)^\top \tilde{y} + d_i + \nu : \tilde{y} \in \mathcal{F}_\tau\} \\ &= \max\{d^\top \tilde{y} + d_i + \nu : \tilde{y} \in \mathcal{F}_\tau\} \\ &\leq \nu \leq \nu_R - \delta^i, \quad \forall i = 1, \dots, \ell. \end{aligned}$$

Here, the first inequality follows from $d \leq 0$ and $\tilde{y} \geq 0$ for any $\tilde{y} \in \mathcal{F}_\tau$. For $i \in \{\ell+1, \dots, k\}$, using the function Ψ defined in (61), we obtain

$$g(\tau_i^{-1}e_i) = \Psi(\tau_i^{-1}e_i, y^i) \leq \frac{\Phi(y^i) + \Phi(\tau_i^{-1}e_i)}{2} \leq \frac{\nu_R - \delta + \omega}{2} \leq \frac{\nu_R + \omega}{2}.$$

where the first inequality follows from (63), and the second is due to the definition of Tuy's cut and ω . \square

D Further Discussion on Konno's Cut

Recall in Section 3.2, we have discussed the generation of the Konno's cut by computing θ_K , and the elements $\{(\theta_K)_i : i = 1, \dots, k\}$ are defined in (38). In this section, we argue that Konno's cut exists and is computable by solving k LP problems, given that $\delta < \nu_R - \nu$.

We first address Remark 4. It was shown in [18] that for each $i \in \{1, \dots, k\}$, $(\theta_K)_i$ can be computed by solving the following LP:

$$\begin{aligned} (\theta_K)_i^{-1} = \min \quad & -d^\top z + (\nu_R - \delta - \nu)z_0 \\ \text{s.t.} \quad & -F^\top z + wz_0 \geq 0 \\ & \tau^\top z - z_0 \geq 0 \\ & (Q_i)^\top z + d_i z_0 = 1 \\ & z \geq 0, \quad z_0 \geq 0. \end{aligned} \tag{75}$$

We refer interested readers to [18, 34] for more details. The pseudo code for the generation of Konno's cut is summarized in Algorithm 5 below.

Next, we demonstrate that even if LP (75) is pathological, $(\theta_K)_i$ is still well-defined under Assumption 1. The first case is when (75) is infeasible, then the optimal value of (75) is $+\infty$, and thus $(\theta_K)_i = 0$. The other pathological case is when the optimal value of (75) is 0, in which case $(\theta_K)_i = +\infty$ and Konno's cut does not exist. However, as long as $\delta < \nu_R - \nu$, such case never occurs. We first note that by $\nu_R - \delta - \nu > 0$, $d \leq 0$, and the constraints $z \geq 0$, $z_0 \geq 0$, the objective of (75) is always nonnegative. Having an optimal value equal to 0 thus implies that there exists an optimal solution (z^*, z_0^*) satisfying $z_0^* = 0$. It follows that $F^\top z^* \leq 0$, $z^* \geq 0$ and $(Q_i)^\top z^* = 1$. In particular, $z^* \neq 0$ is a direction of \mathcal{F} , which contradicts with the boundedness of \mathcal{F} in Assumption 1. We then conclude that each $(\theta_K)_i$ is well-defined for any $\delta < \nu_R - \nu$ under Assumption 1.

Algorithm 5 Konno_Cut

Input: $Q, d, \nu, F, w, \nu_R, \tau, \delta$.

1: **for** $i = 1, \dots, k$ **do**

2: Compute $(\theta_K)_i$ by solving the LP problem (75).

3: **end for**

Output: $\theta_K \in \mathbb{R}_+^k$ such that $\bar{\phi}_{\tau, \theta_K}^K \leq \nu_R - \delta$.

E Generation of Deeper Cuts

In Section 3 it is mentioned that deeper cuts can be generated using a bisection method. Below in Algorithm 6 we attach the pseudo code for generation of those deeper cuts.

Algorithm 6 DNN_Cut

Input: $Q, d, \nu, F, w, \nu_R, \tau, \theta_0, \eta, \delta$.

- 1: $\theta \leftarrow \theta_0$;
- 2: Compute $\bar{\phi}_{\tau, \eta\theta_0}^L$ based on (49);
- 3: **if** $\bar{\phi}_{\tau, \eta\theta_0}^L \leq \nu_R - \delta$ **then**
- 4: $\theta \leftarrow \eta\theta_0$;
- 5: **else**
- 6: Compute $\bar{\phi}_{\tau, \eta\theta_0}^D$ based on (52).
- 7: **if** $\bar{\phi}_{\tau, \eta\theta_0}^D \leq \nu_R - \delta$ **then**
- 8: $\theta \leftarrow \eta\theta_0$;
- 9: **end if**
- 10: **end if**

Output: $\theta \leq \theta_0$ such that $\phi_{\tau, \theta}^* \leq \nu_R - \delta$.

F Supplementary Numerical Results

In addition to the numerical experiments presented in Section 5, we provide more detailed results for **QuadProgCD-G** in this section. Table 7 supplements Table 2 by offering additional information about the algorithm performance on the instances from the real dataset Bio-Data100. Specifically, the table includes the number of iteration performed by **QuadProgCD-G** before convergence or reaching the time limit, and the proportion of wallclock time spent on different tasks. The tasks include the search of KKT points, computation of DNN bounds, performing Konno's cut (Algorithm 5), and performing DNN cuts (Algorithm 6). The same information for datasets PCQMAX and CQMAX is presented in Table 8. According to the tables, the majority of computation efforts is on computing DNN bounds, and generating DNN cuts takes the second place. This is not surprising since these two tasks requires solving several semidefinite programs.

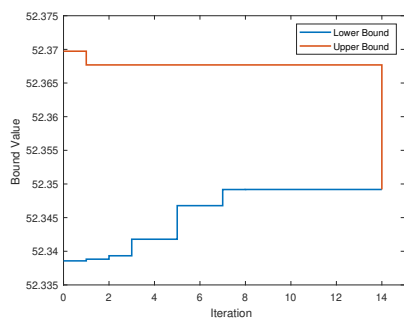
We also test the per-instance variation of the lower and upper objective bounds computed by **QuadProgCD-G** with respect to iteration, as shown in Figure 5. The test instances are chosen to be the same ones as in Figure 4. It can be observed that the upper bound for objective value is *not* decreased for each iteration, meaning that adding a single cut may not reduce the upper bound. Therefore, keeping adding various cuts to the feasible region is necessary for the convergence.

Table 7 Detailed numerical results for **QuadProgCD** on real dataset BioData100. A red instance index means that **QuadProgCD** failed to solve the corresponding instance to the prescribed tolerance ($\epsilon = 10^{-6}$) in the time limit (3600 seconds). The percentages in each row may not add up to 100% due to time spent on pre-processing and post-processing.

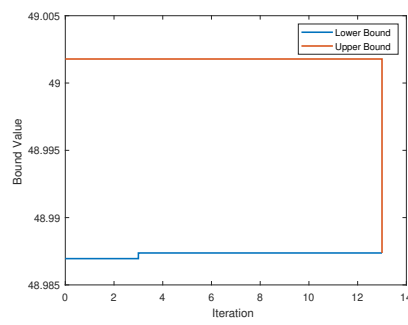
Instance	Iteration	Time			
		KKT Points	DNN Bound	Konno's Cut	DNN Cut
257424	5	0.23%	61.05%	0.64%	38.05%
84896	3	0.28%	93.15%	0.80%	5.74%
141783	3	0.21%	68.57%	0.57%	30.64%
123044	2	0.29%	96.16%	0.60%	2.93%
303256	2	0.32%	93.66%	0.72%	5.28%
312988	37	0.08%	60.27%	0.33%	39.32%
229644	1	0.21%	96.47%	1.09%	2.17%
259490	2	0.28%	93.29%	0.68%	5.73%
143339	2	0.27%	95.16%	0.60%	3.95%
95618	12	0.15%	62.00%	0.56%	37.28%
23659	2	0.27%	95.36%	0.63%	3.71%
284341	2	0.24%	95.11%	0.56%	4.07%
79834	2	0.28%	94.65%	0.61%	4.44%
88552	2	0.25%	98.25%	0.60%	0.88%
305293	6	0.20%	70.23%	0.64%	28.93%
149864	1	0.27%	98.40%	1.29%	0.00%
81426	4	0.19%	73.45%	0.69%	25.65%
274863	4	0.17%	66.34%	0.60%	32.88%
82857	2	0.27%	93.97%	0.60%	5.15%
211213	3	0.26%	92.89%	0.74%	6.09%

Table 8 Detailed numerical results for QuadProgCD on synthetic datasets PCQMAX and CQMAX. The percentages in each row may not add up to 100% due to time spent on pre-processing and post-processing.

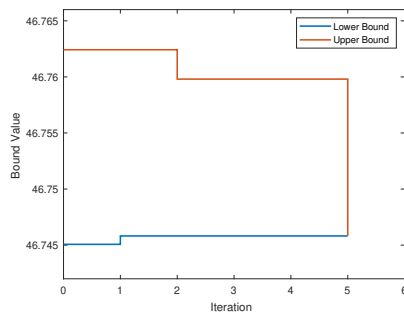
Instance	Iteration	Time			
		KKT Points	DNN Bound	Konno's Cut	DNN Cut
pcqmax20-1	1	44.92%	29.96%	16.78%	0.00%
pcqmax20-2	1	44.06%	16.39%	36.23%	0.00%
pcqmax20-3	2	19.06%	44.73%	23.06%	7.19%
pcqmax20-4	1	11.13%	36.80%	38.89%	5.45%
pcqmax20-5	1	25.83%	62.66%	0.00%	0.00%
pcqmax20-6	1	5.86%	36.42%	52.58%	0.00%
pcqmax20-7	2	16.57%	41.01%	33.90%	3.23%
pcqmax20-8	1	12.17%	37.85%	44.41%	0.00%
pcqmax20-9	1	11.94%	35.74%	47.68%	0.00%
pcqmax20-10	1	11.29%	26.05%	58.34%	0.00%
pcqmax50-1	1	1.98%	83.72%	13.72%	0.00%
pcqmax50-2	1	4.93%	83.86%	10.60%	0.00%
pcqmax50-3	2	3.43%	85.03%	5.77%	5.09%
pcqmax50-4	1	2.17%	75.51%	10.14%	11.18%
pcqmax50-5	2	3.33%	85.05%	6.21%	4.83%
pcqmax50-6	2	5.70%	83.94%	5.74%	4.09%
pcqmax50-7	1	4.29%	95.08%	0.00%	0.00%
pcqmax50-8	1	2.06%	85.78%	11.58%	0.00%
pcqmax50-9	1	11.63%	64.98%	22.78%	0.00%
pcqmax50-10	1	2.47%	67.91%	16.22%	12.46%
pcqmax100-1	2	0.30%	93.86%	0.89%	4.92%
pcqmax100-2	1	0.28%	93.06%	1.36%	5.22%
pcqmax100-3	2	0.62%	94.02%	0.80%	4.54%
pcqmax100-4	2	0.65%	91.62%	0.88%	6.83%
pcqmax100-5	2	0.48%	94.33%	0.81%	4.36%
pcqmax100-6	2	0.69%	95.71%	0.62%	2.95%
pcqmax100-7	3	0.58%	91.75%	1.00%	6.64%
pcqmax100-8	2	0.24%	91.24%	0.87%	7.63%
pcqmax100-9	2	0.67%	96.21%	0.63%	2.46%
pcqmax100-10	2	0.24%	92.82%	0.82%	6.10%
cqmax20-1	1	28.60%	31.66%	35.14%	0.00%
cqmax20-2	1	19.73%	36.85%	39.32%	0.00%
cqmax20-3	1	27.12%	31.25%	37.68%	0.00%
cqmax20-4	1	26.27%	26.16%	43.73%	0.00%
cqmax20-5	1	7.36%	35.53%	51.42%	0.00%
cqmax20-6	1	14.37%	39.98%	41.18%	0.00%
cqmax20-7	1	16.09%	35.26%	35.99%	6.16%
cqmax20-8	1	14.59%	37.36%	43.46%	0.00%
cqmax20-9	1	21.29%	35.86%	38.69%	0.00%
cqmax20-10	1	8.44%	41.69%	45.49%	0.00%
cqmax50-1	1	2.58%	83.90%	12.82%	0.00%
cqmax50-2	1	2.97%	76.89%	12.49%	6.49%
cqmax50-3	1	4.91%	76.77%	11.38%	5.93%
cqmax50-4	1	3.65%	83.82%	11.79%	0.00%
cqmax50-5	2	4.32%	87.41%	4.48%	3.24%
cqmax50-6	2	4.83%	86.43%	5.05%	3.16%
cqmax50-7	2	3.59%	88.31%	5.85%	1.71%
cqmax50-8	2	4.75%	84.07%	5.79%	4.92%
cqmax50-9	1	4.36%	84.58%	10.48%	0.00%
cqmax50-10	1	2.87%	82.76%	13.64%	0.00%
cqmax100-1	2	0.77%	96.69%	0.52%	1.98%
cqmax100-2	1	1.70%	97.04%	1.20%	0.00%
cqmax100-3	2	0.78%	97.11%	0.48%	1.58%
cqmax100-4	2	0.49%	96.93%	0.53%	2.00%
cqmax100-5	1	1.72%	96.86%	1.34%	0.00%
cqmax100-6	3	0.62%	83.99%	0.54%	14.81%
cqmax100-7	2	1.01%	96.54%	0.49%	1.93%
cqmax100-8	3	0.92%	76.25%	0.45%	22.35%
cqmax100-9	3	0.59%	73.98%	0.42%	24.99%
cqmax100-10	2	1.06%	97.14%	0.45%	1.30%



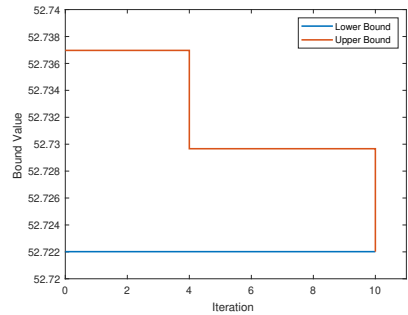
(a) BioData instance 257424.



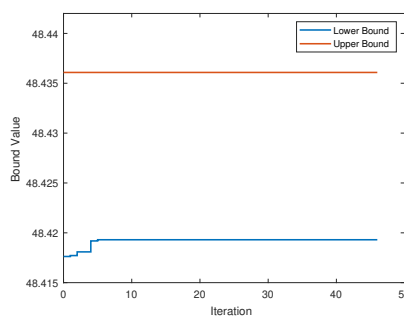
(b) BioData instance 305293.



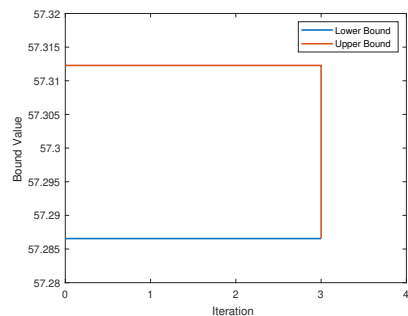
(c) BioData instance 141783.



(d) BioData instance 303256.



(e) BioData instance 312988.



(f) BioData instance 84896.

Fig. 5 Computed lower and upper bounds in each iteration of QuadProgCD.